

Aus der Klinik und Poliklinik für Urologie
(Direktor Univ.- Prof. Dr. Martin Burchardt)
der Universitätsmedizin der Universität Greifswald

Thema:

Evaluating the Impact of NF κ B on the Loss of Apoptosis Induction by TP53 in clear cell
Renal Cell Carcinoma (ccRCC)

Inaugural – Dissertation

zur

Erlangung des akademischen

Grades

Doktor der Medizin

(Dr. med.)

der

Universitätsmedizin

der

Universität Greifswald

2023

vorgelegt von:
Miriam Ophelia Gröber
geb. am: 05.01.1992
in: Bad Homburg v. d. Höhe

Dekan: Prof. Dr. med. habil. Karlhans Endlich

1. Gutachter: PD Dr. Nils Kröger

2. Gutachter: PD Dr. Jennifer Kranz

Ort, Raum: Universitätsmedizin Greifswald, Klinik für Innere Medizin A, Seminarraum
7.0.15/17

Tag der Disputation: 02.04.2024

Contents

List of abbreviations

1. Introduction	1
1.1. Current treatment options	2
1.2. HIF/VHL	2
1.3. P53	4
1.4. NFκB	5
1.5. Aim of the study	7
2. Material and methods	9
2.1. Chemicals and commercial solutions	9
2.2. Buffers and solutions	10
2.3. Antibodies	12
2.4. Instruments	14
2.5. Consumables	15
2.6. Kits	16
2.7. Cell culture	16
2.7.1. Cell lines	16
2.7.2. Media for cell culture	16
2.7.3. Supplements for cell culture	17
2.7.4. Cultivation and passaging	18
2.7.5. Cryopreservation and thawing	18
2.7.6. Irradiation of cells	19
2.7.7. Exposure to hypoxia	19
2.8. Methods of biochemical analysis	20
2.8.1. Protein isolation using CHAPS or RIPA lysis buffer	20
2.8.2. Preparation of nucleic and cytoplasmic extracts	20
2.8.3. Bradford assay	21
2.8.4. SDS Page	21
2.8.5. Western blot	21
2.8.6. rtPCR	22
2.8.7. Statistical analysis	24

3. Results	25
3.1. Characterizing of the cell lines according to their HIF expression pattern	25
3.1.1. HIF-1 α	25
3.1.2. HIF-2 α	26
3.2. Investigation of Mdm2 expression	27
3.3. Evaluating the response of the NF κ B pathway to radiation	29
3.3.1. I κ B α and pI κ B α	29
3.3.2. IKK α/β and pIKK α/β	31
3.3.3. P65, pP65, P105 and P50 in nucleic and cytoplasmic extracts	33
3.3.4. C-Myc	35
3.3.5. cIAP-1, cIAP-2, Bcl-XL	36
3.3.6. Il6	41
4. Discussion	43
4.1. Characterization of the cell lines according to their HIF-1 α and HIF-2 α expression pattern in cytoplasm and nucleus	43
4.2. The behavior of the NF κ B pathway following irradiation with 2 Gy and 10 Gy	
4.2.1. Activation of the NF κ B pathway	44
4.2.2. Crosstalk between the NF κ B pathway and p53	46
4.2.3. Immunological effects of NF κ B pathway	47
4.3. Paragraph of limitations and clinical significance	47
4.4. Summary	49
5. Bibliography	50
6. Eidesstattliche Erklärung	54

List of abbreviations

°C	degree Celsius
μ	micro (10 ⁻⁶)
Bcl	B-cell lymphoma
BSA	Bovine Serum Albumine
ccRCC	Clear cell renal cell carcinoma
CHAPS	3-[(3-Cholamidopropyl) dimethylammonio]-1-propanesulfonate
CREB	cAMP response element-binding protein
DMSO	Dimethyl sulfoxide
DNA	Deoxyribonucleic Acid
dNTP	Deoxynucleoside triphosphate
EDTA	Ethylenediaminetetraacetic acid
EGTA	Egtazic acid
Et al.	and others
Fig.	figure
Gy	Grey
HEPES	4-(2-hydroxyethyl)-1-piperazineethanesulfonic acid
HIF	Hypoxia inducible factor
IAP	Inhibitor of apoptosis
IKK	IκB kinase
IL6	Interleukin 6
IκBα	Nuclear factor of kappa light polypeptide gene enhancer in B-cells inhibitor
KCl	Potassium chloride
l	Litre
LE	Low electroendosmosis
m	milli (10 ⁻³)
Mdm2	Mouse double minute 2 homolog
MgCl ₂	Magnesium chloride
min	minute
NaCl	Sodium chloride
NaF	Sodium fluoride
Na ₃ VO ₄	Sodium orthovanadate
NF-κB	Nuclear factor kappa- light- chain- enhancer of activated B cells
PMSF	Phenylmethylsulfonyl fluoride
PBS	Phosphate buffered saline
SDS	Sodium dodecyl sulfate
RBS	Tris buffered saline
RCF	Relative centrifugal force
RPM	Revolutions per minute
TAE	Tris-acetate-EDTA
TKI	Tyrosine kinase inhibitor
Tris	Tris(hydroxymethyl)aminomethane

V	volt
VEGF	Vascular endothelial growth factor
VHL	Von Hippel- Lindau
wt	wild type

1. Introduction

Kidney cancer is the 13th most frequent cancer worldwide. An estimated 337860 people were diagnosed with kidney cancer in 2012 and 143406 people died of the disease, making it the 16th most deadly cancer in general. (1) In Germany, kidney cancer accounts for about 2.4% of all malignancies in women and 3.8 % of all malignancies in men while being responsible for 2.0 % of cancer related deaths in women and 2.7% of cancer related deaths in men. 5 year relative survival is about 77% for both men and women. (2)

Kidney cancer tends to stay asymptomatic for a long period of time and is often detected incidentally by CT scans or ultrasound scans made for other reasons. If symptomatic, warning signs can include hematuria, abdominal pain or paraneoplastic syndromes.(3) Smoking, high blood pressure, obesity and chronic kidney failure as well as familial predisposition are among the risk factors for developing kidney cancer.(2)

Histologically, kidney cancer can be divided into different entities, with Renal Cell Carcinoma (RCC) being the most frequent entity in adults, accounting for about 96 % of all malignant tumors in the kidney.(2)

RCCs are epithelial tumors derived from the proximal tubule and can again be divided into several subtypes. The three most common subtypes are clear cell RCC (ccRCC, about 75%), papillary RCC (about 10 %) and chromophobe RCC (about 5%). (4, 5)

Efforts to further characterize kidney cancer have long been pursued all over the world. In 1999, the Memorial Sloan-Kettering Cancer Center (MSKCC) risk criteria were first published, which groups renal cell carcinoma into three categories according to their risk profile. These categories are based on clinical criteria and include lactate dehydrogenase, hemoglobin, corrected calcium, Karnofsky performance status and time between diagnosis and start of the first systemic therapy (former INF α treatment).(6, 7) Our study has concentrated on ccRCC as the most frequent of the subtypes mentioned. ccRCC presents itself as a solid, yellow mass, as the cell's cytoplasm is rich of glycogen and lipids. The faster the tumor grows and the bigger it gets, the more hemorrhage and internal necrosis can be found in the sample. (8)

When diagnosed, about 25-30% of the patients already have a metastatic spread, hematogenous spread being more common than lymphatic spread. Metastases are most often found in lung, bone, liver and brain. However, RCC is also known for spreading to

unusual sites such as skin, pancreas, adrenal gland and skeletal muscle. An inferior vena cava thrombus can also often be found in advanced RCC. (8)

1.1. Current treatment options

Therapeutic strategies for RCC are subject to ongoing research. While surgical treatment including partial and radical nephrectomy (open, laparoscopic or robot- assisted surgery) remains the gold standard for localized disease, treatment options for metastasized RCC are still limited.

Systemic chemotherapy and radiotherapy, which are an important part of the therapeutic regimen of most malignant tumors, are not recommended as treatment for RCC, as RCC seems to be resistant against both therapeutic strategies. (9) Key problem amongst others seems to be the deficient induction of apoptosis due to insufficient control mechanisms, which usually lead to controlled cell death. The reason currently remains unclear. (8, 10, 11)

Immunotherapy has been an important part of treatment for progressive RCC and especially ccRCC for many years, including cytokines (IL2) and interferons (INF- α). As of today, they are not recommended as sole treatment for metastasized disease anymore. (9) More recent therapies include tyrosine-kinase inhibitors (TKI) that target the VEGF receptor, such as Sunitinib, mTOR inhibitor Temsirolimus, which suppresses angiogenesis and cell growth and Bevacizumab, a monoclonal antibody that binds and neutralizes VEGF.(12, 13)

These new therapies have brought a prolonged progression free survival as well as a longer overall survival rate. (14)

However, there has been a wide range of response rate and side effects, with no good prognostic factors at hand to select the patients who would benefit from these therapies (15, 16). Molecular markers are needed in order to further classify kidney cancer and especially ccRCC in regard to the new therapy options, in addition, new targets for more treatment options are still urgently called for. (16)

1.2. HIF/ VHL

ccRCC can occur in sporadic or inherited forms. It is especially linked to the von-Hippel-Lindau (VHL) syndrome, where patients have a 70% chance of developing ccRCC in their

lifetime.(17) VHL syndrome is characterized by mutation of the VHL-gene, located at chromosome 3p25-26, which encodes for pVHL. (18)

However, mutation of the VHL gene, which can occur through several different mechanisms such as single nucleotide polymorphism, loss of heterozygosity or methylation not only appears in inherited ccRCC but also in almost all sporadic ccRCCs. On the contrary, it hardly ever appears in other forms of RCC, such as the Papillary or Chromophobe RCC.

Mutation of the VHL- gene seems to take place at the beginning of carcinogenesis, which could make it a very promising target for new therapeutic approaches.(19, 20)

pVHL is part of an E3 ubiquitin ligase complex that can be found in the cytoplasm as well as in the nucleus of a cell.(21) One of its most important functions is targeting the α -subunit of hypoxia-inducible factor (HIF), which consists of an instable α (HIF-1 α or HIF-2 α) and a stable β -subunit. This process can only take place under the impact of oxygen. It eventually leads to the degradation of the HIF- α subunit.

In hypoxic conditions, HIF- α can dimerize with HIF- β and function as a transcription factor for various genes such as GLUT-1, VEGF, PDGF, CXCR4 and EPO. The lack of pVHLwt consequently leads to an overexpression of those genes which amongst others heavily promote angiogenesis. (18, 21)

Both HIF- α subunits function as transcription factors as described above. The set of genes they target however are not completely identical, especially HIF-2 α seems to play a pivotal role in carcinogenesis in comparison to HIF-1 α . Reports have even gone as far as characterizing HIF-1 α as a tumor- suppressor gene and HIF-2 α as an oncogene. (22)

A lot of ccRCCs have been found to solely express HIF-2 α , others express both HIF-1 α and HIF-2 α . Cells that express pVHLwt express neither HIF-1 α nor HIF-2 α permanently. (21)

An important gene, which is promoted by HIF-2 α but suppressed by HIF-1 α is c- Myc (part of the Myc family). It plays an important part in cell cycle progression, cell growth and cell differentiation. An overexpression can lead to less DNA damage repair and thus to an accumulation of mutations. (22, 23)

VHL can also advocate tumorigenesis independently from HIF, by playing an important role in the formation of the extracellular matrix for example. It has also been suggested, that VHL inhibits NF κ B activity, while HIF can activate said pathway. NF κ B in general

exhibits an increased level of activity in most ccRCCs and can lead to an increased transcription of HIF. (21)

A model to further classify ccRCC according to their HIF- α -expression pattern was proposed, giving credit to the importance of said pathway in ccRCC carcinogenesis. VHL deficient tumors, containing both HIF-1 α and HIF-2 α were designated the subtype “H1H2”, tumors only containing HIF-1 α or HIF-2 α were designated the subtype “H1” or “H2” respectively. Tumors containing wild type von-Hippel-Lindau-protein were designated the subtype “VHLwt”. (23)

It has been observed, that tumors of the subtype “H2” tend to be more aggressive and might be associated with a poorer prognosis. (23)

1.3. P53

Tumor suppressor p53 plays a key role in cell cycle arrest and apoptosis induction. It is activated, whenever cells are damaged, and can both initiate cell cycle arrest and DNA repair mechanisms or programmed cell death. There are several pathways that can activate p53. These include activation via DNA damage, for example by ionizing radiation, through kinases ATM and Chk2 and activation via abnormal cell growth signals, for example expression of oncogene c-Myc. The p53 gene is located at chromosome 17. It is found mutated in many cancer forms, including breast- and colon cancer. (24) The function of p53 is closely linked to Mdm2, a protooncogene which can interfere with p53's transcriptional activity as well as export it out of the nucleus. Mdm2 can also function as an ubiquitin ligase, thus leading to the degradation of p53. p53 can escape the regulation of Mdm2 by being phosphorylated by kinases of the p53-activating pathways such as Chk2. (25) Rising levels of p53 in reverse lead to increased transcription of Mdm2, hence creating an autoregulatory feedback-loop. (26) DNA damage will activate the checkpoint inhibitors, which then initiate the phosphorylation of p53. Phosphorylated p53 is more stable and more prone to being transcriptionally active.(27)

Mutation of p53 plays an important part in tumorigenesis across most cancer types. It is probably one of the proteins found to be most often mutated in human cancer. In addition, it is often associated with a poorer prognosis.

ccRCC seems to be an exception to the role, because p53 has been found mutated at an unusually low frequency. (28, 29)

However, the absence of mutations doesn't necessarily mean p53 will function the way it should.

Cervical cancer for example, which is often associated with HPV- infection, is also associated with a low frequency of p53 mutations. Key event in this tumorigenesis seems to be the expression of E6 protein, which leads to the degradation of p53. (30) Such an incident as described above has not been described in ccRCC. On the contrary, several studies have shown an accumulation of functioning p53 in ccRCC, which is in addition associated with a poorer prognosis. (31) Kroeger et al amongst others have shown, that wtp53 is properly activated following proapoptotic signals such as radiation and can be found in the nucleus. However it is not able to induce apoptosis. The mechanism remains unclear and is subject to our ongoing research. (30)

1.4. NFκB

The NFκB pathway is key component of the immune response system but also involved in a variety of other biological processes. It was first discovered in B-cells but has as of today been detected in almost all cell types.(32) It can be activated by a wide range of signals including bacterial products, viruses, inflammatory cytokines, UV- light or γ- radiation and drugs. In response, many genes offer DNA sequences, which can be activated by NFκB. Target genes include not only those involved in the immune response such as IL6 for example but also genes which are involved in apoptosis, cell survival and proliferation. (33, 34)

The NFκB pathway has thus been associated with a several diseases, such as autoimmune disease, cancer and even addiction. (35, 36)

The heart of the NFκB pathway consists of five NFκB proteins – p65 (RelA), RelB, c-Rel, p105/p50 (NF-κB1), and p100/52 (NF-κB2). They all share a Rel- homology domain, which consists of 300 conserved amino acids.(37) This domain is responsible for transcriptional activity, for entering the nucleus and for partnering up with other NFκB- members. (37) The amino- terminal and carboxy- terminal part of the Rel- homology domain both have specific tasks. While the carboxy- terminal part mainly interacts with other members of the NFκB family, the amino- terminal part is amongst others responsible for transcriptional activity. (35)

They NFκB proteins form transcriptionally active homo- or heterodimers. The most frequent heterodimer found is p50/p65, but other options have been described, for

example p50/p50 homodimers. The NFκB dimers are usually kept in the cytosol by an inhibitory protein, typically IκBα, IκBβ or IκBε, which prevents them from entering the nucleus. (32) Precursor proteins p105 and p100 also function as inhibitors. They are processed following activation of an upstream pathway as well as constitutively, resulting in NFκB proteins p50 and p65. (37) An important characteristic of all inhibitory proteins are multiple ankyrin repeats, which camouflage the signal for transferring into the nucleus.(35)

The NFκB inhibitors are phosphorylated by an upstream kinase upon stimulation and degraded following poly-ubiquitylation, setting free the NFκB proteins which can then translocate to the nucleus.

The kinase consists of two catalytic subunits, IKKα and IKKβ, and a regulatory subunit, called IKKγ (NEMO). The IKK complex itself needs to be activated via phosphorylation of two serines of at least one of the kinases. However, whether this mostly takes place by auto phosphorylation or by an upstream kinase remains subject to discussion. (38)

The NFκB proteins themselves are also subject to post-translational modifications. A well-known modification is the phosphorylation of p65 by protein kinase A (PKA), which associates with the NFκB- IκB-complex and phosphorylates a serine residue of p65 following degradation of IκB. This phosphorylation has been found to be essential for most of p65’s transcriptional activity. (39, 40)

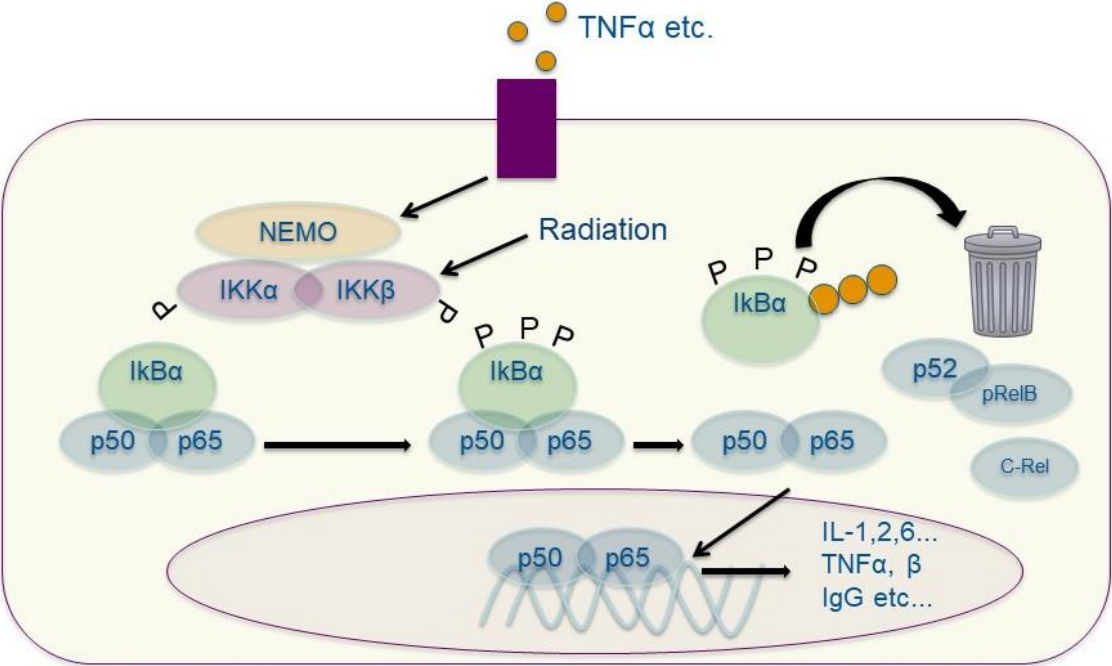


Fig. 1: Simplified representation of the activation of the NFκB pathway.

There is a lot of interaction between NFκB and p53. Both signaling pathways often respond to similar signals and both are involved in the cellular response system to stress of both exogenous and endogenous nature.

The NFκB pathway for example has long been known to function as a transcription factor for p53, working in concert with p53 to induce cell cycle arrest and DNA damage repair when the cell is put under stress. (41) P53 can in return stimulate the NFκB pathway and inhibit the transcription of its inhibitors. (42)

These pathways don't always work in harmony however, as NFκB can also inhibit the induction of apoptosis via p53, for example when activated by TNFα. Tumor cells often retain NFκB which is constitutively active, this has for example been demonstrated in RCC cell lines. In addition, there are strong indicators, that NFκB might be even responsible for the insufficient activation of p53 in RCC. (43) Key element might be several anti-apoptotic target genes, which include IAP family members ciap-1 and ciap-2 and Bcl-2 family member Bcl-Xl.(44-46)

In summary, the role of NFκB must be evaluated in context of the situation it is activated in and the cell it is analyzed in.

1.5. Aim of the study

Patients, who are diagnosed with metastasized ccRCC, face a poor prognosis. Treatment options are still very limited today, because ccRCC is immune to chemo- and radiotherapy.

As prior experiments by Kroeger et al. have shown and as is highlighted above, even though p53 is activated by radiotherapy, apoptosis cannot be induced. The reason remains unclear.

The NFκB pathway is believed to be an important counterpart of apoptosis-inducing mechanisms. It has already been demonstrated, that certain tumor cells, including RCCs, possess constitutively active NFκB. Considering the antiapoptotic qualities of NFκB as described above, investigating into this relationship might provide new insights into tumorigenesis of ccRCC and, especially, targets for new treatment options.

As we gain more insights into molecular pathophysiology of tumorigenesis, differences between tumors of the same entity arise. We believe, that the future lies in the personalization of tumor therapy, where the molecular characterization of a tumor

might predict the prognosis of a patient, the most fitting therapy and maybe possibly even the side effects to be expected.

Our aim was to

1. characterize the ccRCC cell lines 786-O, A-498, CaKi-1, RCC4, CaKi2, UOK-220 and kidney cell line Rc-124 according to their HIF-1 α and HIF-2 α expression pattern in cytoplasm and nucleus and subsequently assign the cell lines to one of the subtypes H2, H1H2 or VHLwt
2. study the behavior of the NF κ B- pathway following irradiation with 2 Gy and 10 Gy
3. Examine the expression of anti- apoptotic target genes ciap-1, ciap-2 and Bcl- XL as well as the expression of IL6
4. examine the possible differences between the ccRCC subtypes in their response to irradiation

2. Materials and Methods

2.1. Chemicals and commercial solutions	
Chemical/ commercial solution	Distributor
Bromphenol blue	Kallie Feinchemie AG, Sebnitz, Germany
BSA	Carl Roth, Karlsruhe, Germany
C ₂ HCl ₃ O ₂	Carl Roth, Karlsruhe, Germany
C ₆ H ₁₆ N ₂	Carl Roth, Karlsruhe, Germany
C ₇ H ₇ F ₀ S	Sigma- Aldrich, Steinheim, Germany
CHAPS	AppliChem, Darmstadt, Germany
CH ₃ CO ₂ K	Carl Roth, Karlsruhe, Germany
Coomassie® Brilliant Blue G 250	Fluka, Buchs, Switzerland
Complete™ Mini, EDTA free	Roche Diagnostics, Mannheim, Germany
DMSO	Carl Roth, Karlsruhe, Germany
dNTP- Mix	Fermentas, St. Leon- Rot, Germany
DTT	AppliChem, Darmstadt, Germany
EDTA	Carl Roth, Karlsruhe, Germany
EGTA	SERVA Electrophoresis GmbH, Heidelberg, Germany
Ethanol (96% pure)	Merck Millipore, Darmstadt, Germany
Glycerol	Carl Roth, Karlsruhe, Germany
Glycerol- 2- phosphate	Sigma- Aldrich, Steinheim, Germany
HEPES	Carl Roth, Karlsruhe, Germany
KCl	Carl Roth, Karlsruhe, Germany
LE Agaroses	Biozym Scientific, Hessisch Oldendorf, Germany

MgCl ₂	Merck Millipore, Darmstadt, Germany
M- MLV Reverse Transcriptase	Promega, Mannheim, Germany
NaCl	Carl Roth, Karlsruhe, Germany
NaF	Sigma- Aldrich, Steinheim, Germany
Na ₃ Vo ₄	Sigma- Aldrich, Steinheim, Germany
Nonidet™ P-40	Sigma- Aldrich, Munich, Germany
NP-40	Sigma- Aldrich, Steinheim, Germany
peqGOLD TriFAST™	PeqLab, Erlangen, Germany
Phosphatase inhibitor cocktail 3	Sigma- Aldrich, Munich, Germany
PMSF Protease inhibitor	Sigma- Aldrich, Steinheim, Germany
Poly-L-Lysine	Sigma- Aldrich, Munich, Germany
Ponceau S	Carl Roth, Karlsruhe, Germany
RiboLock™ RNase- Inhibitor	Fermentas, St. Leon- Rot, Germany
Ribonuclease A	Carl Roth, Karlsruhe, Germany
ROTI® Free Stripping buffer	Carl Roth, Karlsruhe, Germany
SDS	SERVA Electrophoresis, Heidelberg, Germany
Skimmed milk powder	Carl Roth, Karlsruhe, Germany
Tris	Carl Roth, Karlsruhe, Germany
Triton X-100	Ferak, Berlin, Germany
Trypsin	Carl Roth, Karlsruhe, Germany
Tween® 20	Sigma- Aldrich, Steinheim, Germany

2.2. Buffers and solutions

If not stated otherwise, Aqua dest. was used as solvent

10x PBS	1,37 M NaCl; 26,8 mM KCl; 17,6 mM KH ₂ PO ₄ ; 101,1 mM Na ₂ PO ₂ x 2 H ₂ O; pH 7,4
10x Running buffer	192 mM Glycine; 24,8 mM Tris; pH 8,3
1x SDS Running buffer	10% v/v Running buffer; 0,1% v/v 10% SDS
10% SDS	10% w/v SDS- Pellets
10x TBS	0,2 M Tris; 1,5 M NaCl; pH 7,8
1x TBST	10% v/v 10x TBS; 0,1% v/v Tween 20
10x Transfer buffer	0,25 M Tris, 1,9 M Glycine, pH 8,0
1x Transfer buffer	1 VT 10x transfer buffer, 7 VT aqua dest, 2 VT Ethanol
2y Trypsin/EDTA	20% v/v 10x Trypsin/EDTA in DPBS
50x TAE Buffer	2 M Tris; 1,5 M NaCl; pH 7,6
1x TAE Buffer	0,02% v/v 50x TAE
5x Loading buffer	156 mM Tris, pH 6,8; 25% v/v Glycerol; 5% v/v SDS; 12,5% v/v β-Mercaptoethanol; 0,2% w/v bromphenol blue
Antibody solution	5% w/v BSA; 10% v/v 10x TBS; 0,001% v/v Tween 20
Blocking buffer 1	10% v/v Rotiblock 10x concentration
Blocking buffer 2	5% skimmed milk in TBST
Bradford reagent	10% v/v Coomassie Brilliant Blue G 250; 5% v/v Ethanol; 8,5% v/v H ₃ PO ₄
Buffer A	10 mM Tris, pH 7,9; 10 mM KCl; 1,5 mM MgCl ₂ ; 10 % v/v Glycerol, 10 mM K ₂ HPO ₄ ; 1 mM Na ₃ VO ₄ , 10 mM NaF
Buffer C	20 mM Tris, pH 7,9; 0,24 M NaCl; 1,5 mM MgCl ₂ ; 0,2 mM EDTA; 10 % v/v Glycerol; 10 mM K ₂ HPO ₄ ; 1 mM Na ₃ VO ₄ , 10 mM NaF
CASY ton	154 mM NaCl, 0,1 mM EDTA

CHAPS extraction buffer	CHAPS lysis buffer, pH 7.5: 150 mM NaCl, 50 mM Tris, 1% w/v CHAPS Triton lysis buffer: 25 mM HEPES, 300 mM NaCl, 1.5 mM MgCl ₂ , 2 mM EDTA, 2 mM EGTA, 10 % Glycerol, 1 % Triton X-100
Developing solution S1	100 mM Tris-HCl pH 8.5, 24.8 mM Luminol, 9.1 mM p-coumaric acid
Developing solution S2	S2: 100 mM Tris-HCl pH 8.5, 0.018% v/v H ₂ O ₂
Lysis buffer stock solution (RIPA)	50 mM Tris; pH 7,5; 5 mM EDTA; pH 8,0; 150 mM NaCl; 10 mM K ₂ HPO ₄ ; 10% v/v Glycerol; 1% v/v Triton X-100; 0,05% v/v SDS
Lysis buffer working solution	67% RIPA stock solution, 1mM SV, 20 mM NaF, 20 mM 2- Glycerophosphat, 0,1 mM PMSF, 20% w/v Complete™ Mini EDTA-free
Mdm2- lysis buffer	25 mM HEPES, 300 mM NaCl, 1,5 mM MgCL ₂ , 2 mM EDTA, 2 mM EGTA, 1 mM DTT, 10 % v/v Glycerol, 1% v/v Triton X-100, 10 mM 2- Glycerophosphat, 25 mM NaF, 1:100 Protease- Inhibitor (Sigma)
Ponceau- S	0,2% w/v Ponceau S, 3% C ₂ HCl ₃ O ₂
Transfer buffer	20% v/v Methanol, 10% v/v running buffer stock solution

2.3. Antibodies

Antibody	Company	Dilution	Source
Anti-HIF-1 α	BD, Franklin Lakes, USA	1:1000	Mouse

Anti-HIF-2 α	Novus Biologicals, Littleton, USA	1:2000	Rabbit
Anti-I κ B α	Cell Signaling, Danvers, USA	1:1000	Rabbit
Anti-IKK α/β	Cell Signaling, Danvers, USA	1:1000	Rabbit
Anti-Mdm2	Sigma	1:2000	Mouse
Anti-NF κ B1 (anti- p105/p50)	Cell Signaling, Danvers, USA	1:1000	Rabbit
Anti-NF κ B2 (anti- p100/p52)	Cell Signaling, Danvers, USA	1:1000	Rabbit
Anti-p65	Cell Signaling, Danvers, USA	1:1000	Rabbit
Anti-phospho-I κ B α	Cell Signaling, Danvers, USA	1:1000	Mouse
Anti-phospho-IKK α/β	Cell Signaling, Danvers, USA	1:500	Rabbit
Anti-phospho-p65	Cell Signaling, Danvers, USA	1:500	Rabbit
Anti-phospho-RelB	Cell Signaling, Danvers, USA	1:1000	Rabbit
Anti-c-Rel	Cell Signaling, Danvers, USA	1:1000	Rabbit
Anti-RANK	R&D	1:1000	Mouse
Anti- CREB	Cell Signaling, Danvers, USA	1:1000	Rabbit
Anti- Tubulin	Abcam	1:50000	Mouse

Primer	Primersequenz
c- Myc forward primer	5'-AATGAAAAGGCCCCCAAGGTAGTTATCC- 3'
c- Myc reverse primer	5'-GTCGTTTCCGCAACAAGTCCTCTTC- 3'

clAP-1 forward primer	5'- AGCTAGTCTGGGATCCACCTC- 3'
clAP-1 reverse primer	5'- GGGGTTAGTCCTCGATGAAG- 3'
clAP-2 forward primer	5'- TGGAAGCTACCTCTCAGCCTAC- 3'
clAP-2 reverse primer	5'- GGAACTTCTCATCAAGGCAGA- 3'
Bcl- XL forward primer	5'- CGGTACCGGCGGGCATTTCAG- 3'
Bcl- XL reverse primer	5'- CGGCTCTCGGCTGCTGCATT- 3'
IL6 forward primer	5'- ACAGCCACTCACCTCTTCAG- 3'
IL6 reverse primer	5'- CCATCTTTTTCAGCCATCTTT- 3'

2.4. Instruments	
Casy TT Cell Counter and Analyzer 150 µm	Roche Diagnostics Germany GmbH
Cell scraper 25 mm	Sarstedt, Nümbrecht, Germany
Centrifuge 5810	Eppendorf, Hamburg, Germany
Centrifuge 5415	Eppendorf, Hamburg, Germany
ChemiDoc™ XRS+	Bio-Rad, Munich, Germany
Clean Bench SAFE 2020	Thermo Scientific, Waltham, USA
Criterion™ Cell	Bio- Rad, Munich, Germany
Incubator CO ₂ - Cell	MMM Medcenter GmbH, Munich, Germany
Ice Flace machine KF 85	Migel (Milan, Italy)
Incubator CB210	Binder (Tuttlingen, Germany)
KC300 sterling nitrile exam gloves	Kimberly-Clark, Roswell, USA
Magnetic stirrer	Carl Roth, Karlsruhe, Germany
Microcentrifuge 5415R	Eppendorf, Hamburg, Germany
Mini Trans-Blot® Cell	Bio-Rad, Munich, Germany
Nano- Drop 2000c	Thermo Scientific, Wilmington, USA
PeqMate pipette	Peqlab Biotechnologie GmbH, Erlangen, Germany
pH meter	Denver Instrument, Göttingen, Germany
Power Supply PowerPack™	Bio-Rad, München
Rotilabo® Mikrozentrifuge	Carl Roth, Karlsruhe, Germany

Scale	KERN& Sohn GmbH
Thermocycler T3000	Biometra, Göttingen
Trans-Blot® SD semi-dry transfer cell	Bio- Rad, München
Vacuum pump VACUSAFE	Integra Bioscience AG, Switzerland
Vibramax 100	Heidolph Instruments, Schwabach, Germany
Water quench	Memmert
Zeiss Observer Z.1	Carl Zeiss AG, Oberkochen

2.5. Consumables	
6 Well Cell Culture Plate	Sarstedt, Nümbrecht, Germany
96 Well Microplate	Sarstedt, Nümbrecht, Germany
96 Well Microplate, transparent	Greiner Bio One
96 Well Microplate, white	Greiner Bio One
Capillary tips MultiFlex Round Tip	Bioscience, Salt Lake City, USA
Cell culture dish 100x200 mm	Sarstedt, Nümbrecht, Germany
Cell culture cultivation flask T25	Sarstedt, Nümbrecht, Germany
Cell culture cultivation flask T75	Sarstedt, Nümbrecht, Germany
Conical centrifuge tube, 15 ml	Sarstedt, Nümbrecht, Germany
Conical centrifuge tube, 50 ml	Sarstedt, Nümbrecht, Germany
Criterion™ TGX™ Precast Gels 26- Well	Bio-Rad, Munich, Germany
Cryopreservation tubes (2 ml)	Sarstedt, Nümbrecht, Germany
Eppendorf tube 1,5 ml	Sarstedt, Nümbrecht, Germany
Filter paper	Whatman, Dassel
Filtertips SafeSeal Tips Professional	Biozym Scientific, Hessisch Oldendorf
Nitril gloves Micro-Touch® Nitra-Tex®	Ansell Healthcare, Brüssel, Belgium
Pasteur pipette made of glass	VWR International, Darmstadt, Germany
Pipette tips (1000 µl, 200µl, 10 µl, 2.5 µl)	Sarstedt, Nümbrecht, Germany
Serological pipettes (1 ml, 2 ml, 5 ml, 10 ml, 25 ml)	Sarstedt, Nümbrecht, Germany
Tissue culture flask 75 cm ²	Sarstedt, Nümbrecht, Germany
Tissue culture flask 175 cm ²	Sarstedt, Nümbrecht, Germany

2.6. Kits	
Prestained Protein Ladder “Dual Color Standards”	Bio-Rad, Munich, Germany
Sensimix SYBR™ Hi-ROX	Bioline, Luckenwalde, Germany
Super Signal® West Femto Maximum Sensitivity Substrate	Thermo Scientific, Waltham, USA
Super Signal® West Pico Chemiluminescent Substrate	Thermo Scientific, Waltham, USA
TGX FastCast Acrylamide Solutions	Bio-Rad, Munich, Germany
Trans-Blot® Turbo RTA Mini PVDF Transfer Kit	Bio-Rad, Munich, Germany

2.7. Cell culture

Cell lines	
2.7.1. Cell line	Distributor
786-0	CLS Cell Lines Service GmbH, Eppelheim
A-498	CLS Cell Lines Service GmbH, Eppelheim
CaKi-1	CLS Cell Lines Service GmbH, Eppelheim
CaKi-2	CLS Cell Lines Service GmbH, Eppelheim
HEK-293	CLS Cell Lines Service GmbH, Eppelheim
RC-124	CLS Cell Lines Service GmbH, Eppelheim
RCC4	HPA, Public Health England, Distributer Sigma Aldrich
SAOS-2	CLS Cell Lines Service GmbH, Eppelheim
UOK-220	Kind gift of Marston Linehan, National Institut of Health Bethesda, Maryland, USA

2.7.2. Media for cell culture

Medium	Supplements	Cell Line	Distributor
DMEM, high glucose	10% FBS 1% Penicillin- Streptomycin 1% Sodium Pyruvate 1% MEM Non- Essential Amino Acids (NEAA)	UOK-220	PAN Biotech, Aidenbach
DMEM, low glucose	10% FBS 1% Penicillin- Streptomycin 0,5 mg/ml G-418	RCC4	PAN Biotech, Aidenbach
McCoy's 5a Medium Modified	10% FBS 1% Penicillin- Streptomycin	RC-124	PAN Biotech, Aidenbach
MEM Eagle	10% FBS 1% Penicillin- Streptomycin 1% Sodium Pyruvate	A-498, CaKi-1	PAN Biotech, Aidenbach
RPMI 1640	10% FBS 1% Penicillin- Streptomycin	CaKi-2, 786-0, SAOS-2, HEK- 293	PAN Biotech Aidenbach

2.7.3. Supplements for cell culture	
Supplement	Distributor/ Composition
DPBS	PAN Biotech, Aidenbach
2x Trypsin/EDTA	20% v/v Trypsin/EDTA (10x) in DPBS
Fetal Bovine Serum (FBS)	PAN Biotech, Aidenbach
Geneticin disulfate (G418)	Carl Roth, Karlsruhe
MEM Non-Essential Amino Acids (NEAA)	PAN Biotech, Aidenbach

Penicillin-Streptomycin	PAN Biotech, Aidenbach
Sodium Pyruvate	PAN Biotech, Aidenbach

2.7.4. Cell cultivation and passaging

All cell lines showed an epithelial morphology and were cultivated in T75-flasks in a humidified atmosphere at 37°C and 5% CO₂. Passaging was performed twice a week and each time, cells were splitted between 1:2 and 1:8, depending on the cell line, at about 90% confluence. For passaging of cell lines 786-O, A-498, RCC4, RC-124, CaKi-2 and UOK-220, medium was aspirated and cells were washed with 2,5 ml of DPBS. 1 ml of 2x Trypsin was added and the tissue culture flasks were incubated at 37°C for 3 minutes, resulting in the detachment of the cells. Rich medium was added according to ratio and 1 ml of cell suspension was transferred to a new tissue culture flask containing fresh medium. The overall amount of medium in T75-flasks added up to 20 ml. 200 µl of G418 were added to the medium of cell line RCC4.

For passaging of cell line CaKi-1, cells were washed with 2,5 ml of DPBS, which was then collected in a 50 ml conical centrifuge tube. 1 ml of Trypsin was added and cells were incubated at 37°C for 3 minutes. The detached cells were transferred to the tube as well and centrifuged for 5 minutes at 1000 rcf. The pellet was suspended in medium and transferred to a T75 flask for cultivation.

2.7.5. Cryopreservation and thawing

Cryopreservation was used for permanent storage of cells at an early passage.

For this purpose, cells were cultivated in T75-flasks and harvested using 2x Trypsin. The cell suspension was then transferred to a 50 ml conical centrifuge tube and rich medium was added. The tube was centrifuged at 1000 rcf and the remaining pellet resuspended in freezing medium. Cells were counted using the CASY Model TT System. Cell-suspension containing 3×10^6 cells was transferred to a cryogenic tube and placed in a freezing container rack at -80°C for 24 hours before being stored at -130°C for long-term storage.

For thawing, the cryogenic tube was placed in a 37°C water bath for 30 seconds. Cells were then suspended in rich medium and pelleted at 1000 rcf for 5 minutes. The supernatant was removed and the cells transferred to T75-flasks for further cultivation.

2.7.6. Irradiation of cells

Irradiation of cells was performed at the Clinic for Radiotherapy and Radiation Oncology, University of medicine Greifswald, in cooperation with Dr. rer. nat. Frank Adler.

Based on results from kinetics determined in previous experiments of our group, a defined amount of cells was seeded either on dishes or in T75-flasks, depending on the harvesting method of choice. Seeding in T75-flasks and seeding of the cell lines A-498 and RC-124 on Poly-L-Lysine-coated dishes was performed three days prior to radiation, seeding of the cell lines 786-O, CaKi-1, RCC4, CaKi-2 and UOK-220 on Poly-L-Lysine-coated dishes was performed two days prior to radiation. For treatment, cells were transported to the Institute of Radiation Medicine using styrofoam boxes. All control groups underwent the same procedure. Treatment consisted of irradiation with either 2 Gy or 10 Gy. Cell cultivation was continued afterwards for a predefined period of time depending on the experiment. The harvesting method used depended on the experiment. Cells were either harvested using trypsin or with a cell scraper.

2.7.7. Exposure to hypoxia

Exposure to hypoxia was performed at the Institute for Medical Biochemistry and Molecular Biology, University of Medicine Greifswald, in cooperation with PD Dr. rer. nat. habil. Horst Lillig.

Cell lines A-498 and RC-124 were seeded on Poly-L-Lysine-coated 100 mm² dishes three days prior to treatment, cell lines 786-O, CaKi-1, RCC4, CaKi-2 and UOK-220 were seeded on Poly-L-Lysine-coated 100 mm² dishes two days prior to treatment. Cells were transported to the hypoxia chamber using a styrofoam box. Control groups underwent similar treatment except exposure to hypoxia. They were then exposed to hypoxia (1% O₂, 5% CO₂) for 16 hours and harvested right afterwards. The harvesting method depended on the structures analyzed in the course of the experiment.

2.8. Methods of biochemical analysis

2.8.1. Protein isolation using CHAPS or RIPA lysis buffer

Cells were harvested as described in 2.6.4 two and eight hours following irradiation. The pellet was suspended in 1 ml DPBS, transferred to a 1.5 ml tube and centrifuged at 1000 rpm for 5 minutes. The supernatant was discarded and the remaining pellet was suspended in the respective amount of CHAPS lysis buffer or RIPA lysis buffer, depending on the proteins analyzed. Protease inhibitor and, if needed, phosphatase inhibitor was added. The suspension was incubated on ice at room temperature for 20 min and afterwards deep frosted at -80 ° C for at least 24 hours. It was then thawed on ice and centrifuged at 14000 rpm for 20 min at 4 ° C. The supernatant was transferred to a new tube and the remaining pellet was discharged.

2.8.2. Preparation of nucleic and cytoplasmic extracts

To prepare nucleic and cytoplasmic extracts, two different buffers (Buffer A, Buffer C) were required. Cells were seeded either on 60 mm dishes or 100 mm dishes coated with Poly-L-Lysine two to three days prior to use.

For harvesting, dishes were placed on ice and medium was aspirated using a vacuum pump. Cells were washed with PBS twice and afterwards covered with Buffer A, using 100 µl per 60 mm plate and 300 µl per 100 mm plate. Cells were then removed using a cell scraper and transferred to a 1.5 ml tube. 1,5 µl Nonidet P-40 (12,5 %) per 60 mm plate or 3 µl Nonidet P-40 (12,5 %) per 100 mm plate was added and cells were incubated on ice for 5 minutes, leading to the disassembly of the cell membrane. The suspension was centrifuged for 10 min (1000 rcf, 4°C) and the supernatant containing the cytoplasmic extract was removed and stored at -20°C for later use. The remaining pellet was resuspended in 15 µl of Buffer C per 60 mm plate or 40 µl of buffer C per 100 mm plate and again centrifuged for 10min (12000 rcf, 4°C). The supernatant containing the nucleic extracts was collected and stored at -20°C as well. The pellet remaining in the tube consisting of cell components and debris of the nuclear membrane was discarded.

2.8.3. Bradford essay

Bradford essay was used to determine the protein concentration of the samples. The binding of Coomassie Brilliant Blue 250 g to proteins results in absorbance change.

Samples were thawed on ice and centrifuged at 14000 rpm and 4°C for 20 min. The supernatant was transferred to a new 1.5 ml tube, dilutions with TE buffer were prepared. 5 μ l diluted sample and bsa standard ranging from 0-0.8 mg/ml were pipetted twice into 96 well plates. 195 μ l bradford was added. The plate was incubated for 10 min in the dark. The absorbance was measured at 595 nm against blank value (reference wavelength at 360 nm). The concentration was calculated using a calibration curve and software libre office calc and xmgrace.

2.8.4. SDS- Page

Sodium dodecyl sulfate polyacrylamide gel electrophoresis (SDS Page) is a method to separate proteins according to their molecular weight. First, the protein concentration was determined using the Bradford essay. The samples were diluted with aqua dest. The amount of protein differed between 20 and 100 μ g depending on the experiment. Then 5x running buffer was added. The sample was heated at 95°C for 5 minutes and then put on ice.

The sample was loaded on 4-20% polyacrylamide gradient gels. Next to the samples a prestained marker was loaded to estimate the molecular weight of the protein analyzed. The proteins were separated using the Mini protean Tetra system for 10 min at 100 V and then for about an hour at 170 V or until the running buffer had reached the bottom of the gel.

2.8.5. Western blot

Following SDS- Page, the proteins were transferred to a PVDF- membrane via Western Blot. For this purpose, the Trans-Blot® Turbo RTA Transfer Kit and PVDF membranes were used. Before blotting, the membranes were activated in 96% pure ethanol, cleaned with aqua dest. and balanced in 1x transfer buffer. 3 filter papers were as well equilibrated in transfer buffer. The gel from SDS- Page was removed from the electrophoresis chamber and kept in transfer buffer.

The blot was then assembled as following: cathode, transfer sponge, 2 filter papers, gel, PVDF membrane, 1 filter paper, transfer sponge, anode.

The transfer was carried out at 30 V for 1h. Afterwards, to estimate the total protein content of the probe, a stain free picture was taken using the ChemiDoc™ XRS+. The membrane was then blocked in skimmed milk for 1-3 hours, washed with TBST and incubated with the primary antibody over night at 4°C. The primary antibody was usually diluted in blocking buffer 1.

The next day, the membrane was washed three times for ten minutes with TBST and then incubated with the secondary antibody for one hour at room temperature, which was diluted in blocking buffer 2. Afterwards, the membrane was again washed with TBST three times for about 10 minutes to remove the secondary antibody.

For development, ChemiDoc™ XRS+ was used. Depending on the signal that was expected, either a mix of development solution S1 and S2 was used or, when a weak substrate was to be expected, a mixture of Super Signal® West Pico Chemiluminescent Substrate and Super Signal® West Femto Maximum Sensitivity Substrate.

The membrane could be washed, blocked for an hour in blocking buffer and then reused by proceeding as stated above.

As some proteins analyzed were difficult to detect, several changes to the protocol had to be made. The blocking buffer for phosphorylated proteins pIκBα, pIKKα/β and pP65 was changed from skimmed milk to 5% BSA, as the casein in skimmed milk can interfere with phosphorylated antibodies. The antibody dilution buffer was changed to 1x Roti for the same reasons.

Harvesting conditions were changed as well, for example using a cell scraper for removal of the cells was exchanged in favor of the sole use of trypsin (for protein isolation, for RNA isolation, a cell scraper was used).

2.8.6. rtPCR

RNA isolation

RNA isolation was done by using the Trizol™ reagent, which helps to break down cells while protecting RNA integrity.

For RNA isolation, cells were cultivated in 6 well cell culture plates. For preparation, the medium was removed and cells were washed with 3 ml of PBS. Afterwards, 500 µl of Trizol was added and cells were incubated for five minutes at room temperature. They were then removed from the surface of the culture plates by using a cell scraper and

transferred into 1,5 ml Eppendorf tubes. 50 µl of 1-Bromo-3-chloropropane was added, the precipitation solution was vortexed for 15 seconds and afterwards inverted for 5 minutes at room temperature. The samples were then centrifuged at 12000 U/min for 15 minutes at 4°C. This step resulted in a separation of the sample into three phases which included DNA, RNA and proteins (from top to bottom). The RNA was transferred into sterile 1,5 ml eppendorf tubes and 250 µl of isopropanolol was added. The sample was inverted 10 times and incubated for 10 minutes at room temperature. It was then centrifuged at 12000 U/min for 10 minutes at 4°C. The supernatant was discarded and the remaining RNA pellet was washed with 500 µl of ethanol. It was then centrifuged at 7500 U/min for 5 minutes at 4°C. The supernatant was discarded and the RNA air dried for 5-10 minutes. It was then dissolved in 32 µl of DEPC-H₂O (RNase free), resuspended and incubated at room temperature for 30 minutes. RNA concentration was determined by using the spectrophotometer Nano- Drop.

Reverse Transcription

Reverse transcription is used to create cDNA by using an RNA template.

First, RNA strands are denatured, then Oligo- dT- Primer bind to the Poly-A- part of the RNA.

We used 1 µg of RNA and 1 µg of Oligo- dT- Primer and added H₂O (RNase free) to get a final volume of 13,25 µl. The sample was incubated at 65 °C for five minutes. Afterwards, a mix consisting of reaction- buffer, dNTP (1 µl of adenine, guanine, cytosine and thymin each), 0,5 µl RNase- inhibitor RiboLock™, and 0,8 µl of M- MLV reverse transcriptase was added. cDNA synthesis was then carried out at 42°C for 1 hour. Afterwards, 280 µl of DEPC water was added and samples were stored at -20°C.

Real- time polymerase chain reaction (rtPCR)

Real- time polymerase chain reaction is used to amplify specific DNA sequences to measure the amount of RNA of the target of interest in the sample.

The cycles of PCR always consist of the same routine. Denaturation leads to the separation of double strands. It is followed by “Annealing”, which means that a specific primer attaches to the complementary sequence of the cDNA. The complementary strand is then synthesized by the enzyme polymerase; this phase is called “Elongation”. Afterwards, the cycle starts from the beginning until reagents are used up.

We used 3 µl of cDNA, 10 µl of SensiMix™ SYBR, 1 µl of reverse and forward primer each and added 5 µl of water. The SYBR- Green in the SensiMix™ SYBR binds to DNA, absorbs 497 nm blue light and emits 520 nm green light. Thus, the amount of cDNA in the sample can be calculated.

denaturation took place for 3 minutes at 95°C, annealing at 65°C for 30 sec., and elongation at 72 °C for 2-3 minutes. A cycle was usually repeated for 29 times.

The relative amount of cDNA of a certain target in the sample was measured against reference gene RPLP0.

The whole procedure was followed by melting curve analysis to detect unspecific pcr products with an aberrant length, as they have a different melting point.

2.8.7 Statistical analysis

The software Microsoft Excel 2010 was used for the statistical evaluation of the collected data. The figures are averages of the results with standard error of the mean (SEM).

3. Results

3.1. Characterizing of the cell lines according to their HIF expression pattern

The cell lines 786-O, A-498, CaKi-1, RCC4, CaKi-2, UOK-220 and Rc-124 were characterized according to their HIF-1 α and HIF-2 α expression pattern in cytoplasm and nucleus. For this purpose, methods mentioned above were used (chapter 2.8.2.).

3.1.1 HIF-1 α

HIF-1 α has a mass of approximately 120 kDa and was detected at the corresponding region.

Before and after exposure to hypoxia, HIF-1 α was observed in the nuclei of cell lines RCC4, CaKi-2 and UOK-220.

No measurable amount of HIF-1 α was detected in the cytoplasm of any cell line before exposure to hypoxia. After exposure, a small amount was observed in cell lines RCC4 and CaKi-2.

We concluded, that cell lines RCC4, CaKi-2 and UOK-220 contain HIF-1 α and that HIF-1 α is mainly found in the nucleus. This might suggest high transcriptional activity of HIF-1 α . The results are depicted in fig. 2.

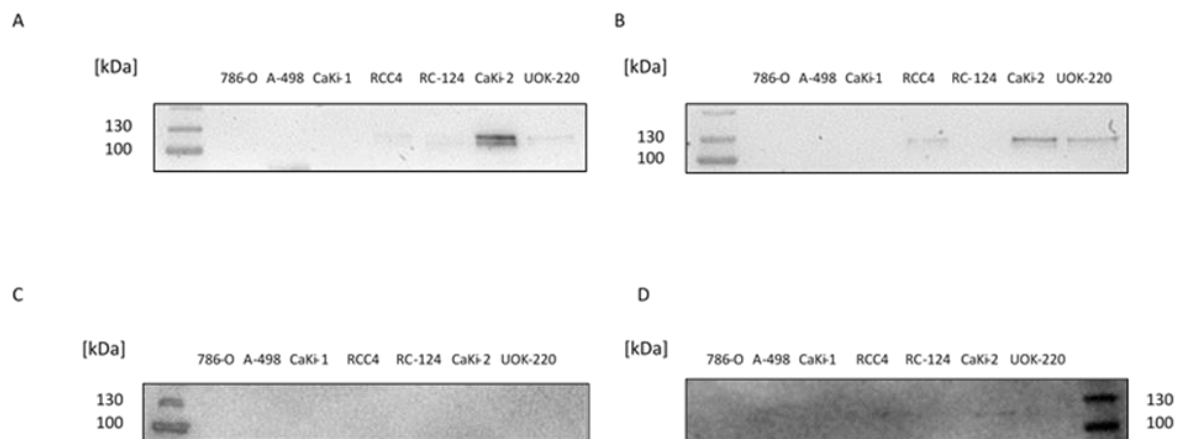


Fig. 2: Western blot demonstrating HIF-1 α expression in the nucleic fraction of ccRCC cell lines (A) in unexposed cells and (B) after exposure to hypoxia and in the cytoplasmatic fraction of ccRCC cell lines (C) in unexposed cells and (D) after exposure to hypoxia.

3.1.2 HIF-2 α

HIF-2 α has a mass of approximately 118 kDa and was detected at the corresponding region.

In the control group of the nucleic fraction, HIF-2 α was observed in cell lines 786-O, A-498, RCC4, and UOK-220. Following exposure to hypoxia HIF-2 α was found in the nucleic fraction of cell lines 786-O, A-498, RCC4, UOK-220 and CaKi-2.

The control group of the cytoplasmatic fraction showed HIF-2 α staining in cell lines 786-O, A-498, and UOK-220. After exposure to hypoxia, HIF-2 α was found in the cytoplasmic fractions of the cell lines 786-O, A-498, RCC4 and UOK-220.

We concluded that cell lines 786-O, A-498, RCC4, UOK-220 and CaKi-2 contain HIF-2 α and that it is mainly found in the nucleus. The western blots are depicted in fig. 3.

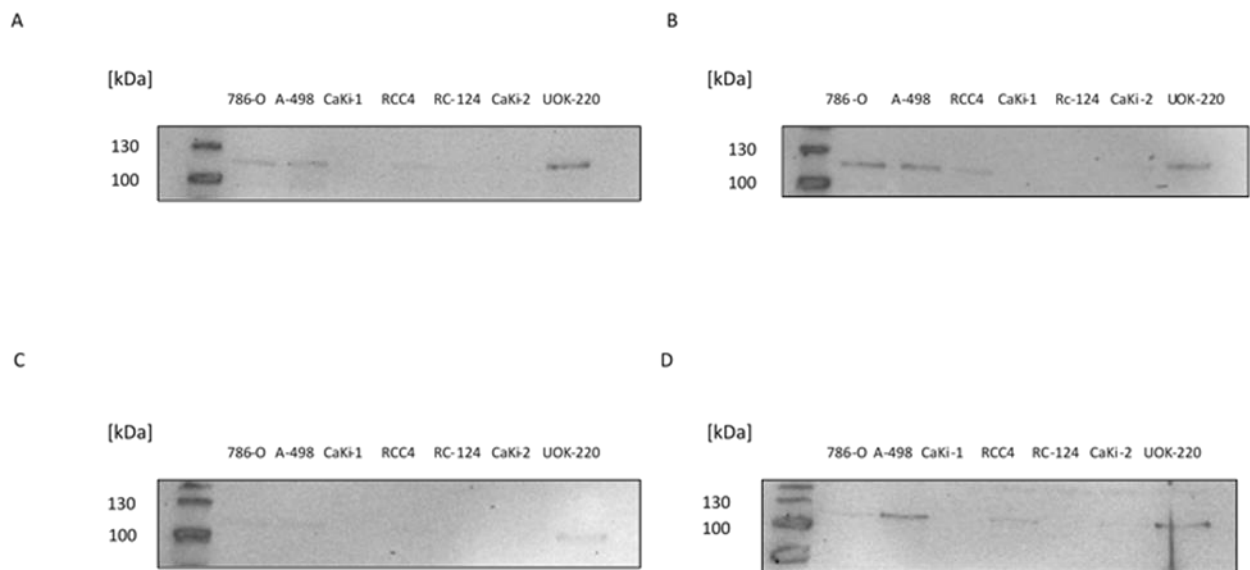


Fig. 3: Western blot demonstrating HIF-2 α expression in the nucleic fraction of ccRCC cell lines (A) in unexposed cells and (B) after exposure to hypoxia and in the cytoplasmatic fraction of ccRCC cell lines (C) in unexposed cells and (D) after exposure to hypoxia.

Our results are depicted in Tbl. 1: Cell lines who express HIF-1 α and HIF-2 α belong to subtype H1H2, cell lines who solely express HIF-2 α belong to subtype H2. Cell lines belonging to VHLwt have wild type VHL alleles (23) and show neither HIF-1 α nor HIF-2 α expression. Three cell lines belong to subtype H1H2 (RCC4, UOK-220, CaKi-2), two cell lines belong to subtype H2 (786-O, A-498) and the remaining cell lines CaKi-1 and Rc-124 did not demonstrate either HIF subunit expression. We used this subclassification of the cell lines in the following experiments.

		ccRCC- subtype			
		H1	H1H2	H2	VHLwt
HIF-member	HIF-1 α	x	x		
	HIF-2 α		x	x	
Cell lines			RCC4, UOK-220, CaKi-2	786-O, A-498	CaKi-1, Rc-124

Tbl. 1: Characterizing of the ccRCC cell lines resulting from the detection of HIF-1 α and/or HIF-2 α in the nucleus via Western Blot.

3.2. Investigation of Mdm2 expression

Mdm2 expression was investigated following irradiation with 2 Gy and 10 Gy via western blots by using the semi-dry transfer system.

After irradiation with 2 Gy, cell lines 786-O, A-498, CaKi-1, RCC-4, Rc-124 and UOK-220 showed an increase in Mdm2 expression compared to untreated cells. Only CaKi-2 showed a slight decrease in Mdm2 expression.

In a second experiment, the cell lines were irradiated with 10 Gy. Cell lines 786-O, CaKi-1, RCC4 and UOK-220 showed an increase in Mdm2 expression, while A-498, Rc-124 and CaKi-2 showed a decrease in Mdm2 expression. Therefore, 2 out of 3 cell lines belonging to subtype H1H2 demonstrated an increase in Mdm2 expression, as well as H2 cell line 786-O and VHLwt cell line CaKi-2.

Previous experiments conducted by Kroeger et. al had shown an increase in p53 expression in ccRCC cell lines following irradiation and the lack of induction of apoptosis. However, they had already noticed some problems with the dosage of 10 Gy inducing necrosis in part of the cells and thus recommended reducing the dosage in the future for further experiments. Our aim was to compare experiments using a lower dosage to experiments conducted with irradiation of 10 Gy.

After irradiation with 2 Gy, the physiological response of Mdm2 to elevated p53 could be witnessed in all cell lines except for CaKi-2 (which showed a slight decrease), demonstrating a functioning feedback loop.

After irradiation with 10 Gy, four out of seven cell lines showed a decrease in Mdm2.

This could be a sign of degradation following for example polyubiquitylation. Mdm2 is

capable of self- polyubiquitylation and can in this manner be degraded. The results are depicted in fig. 4.

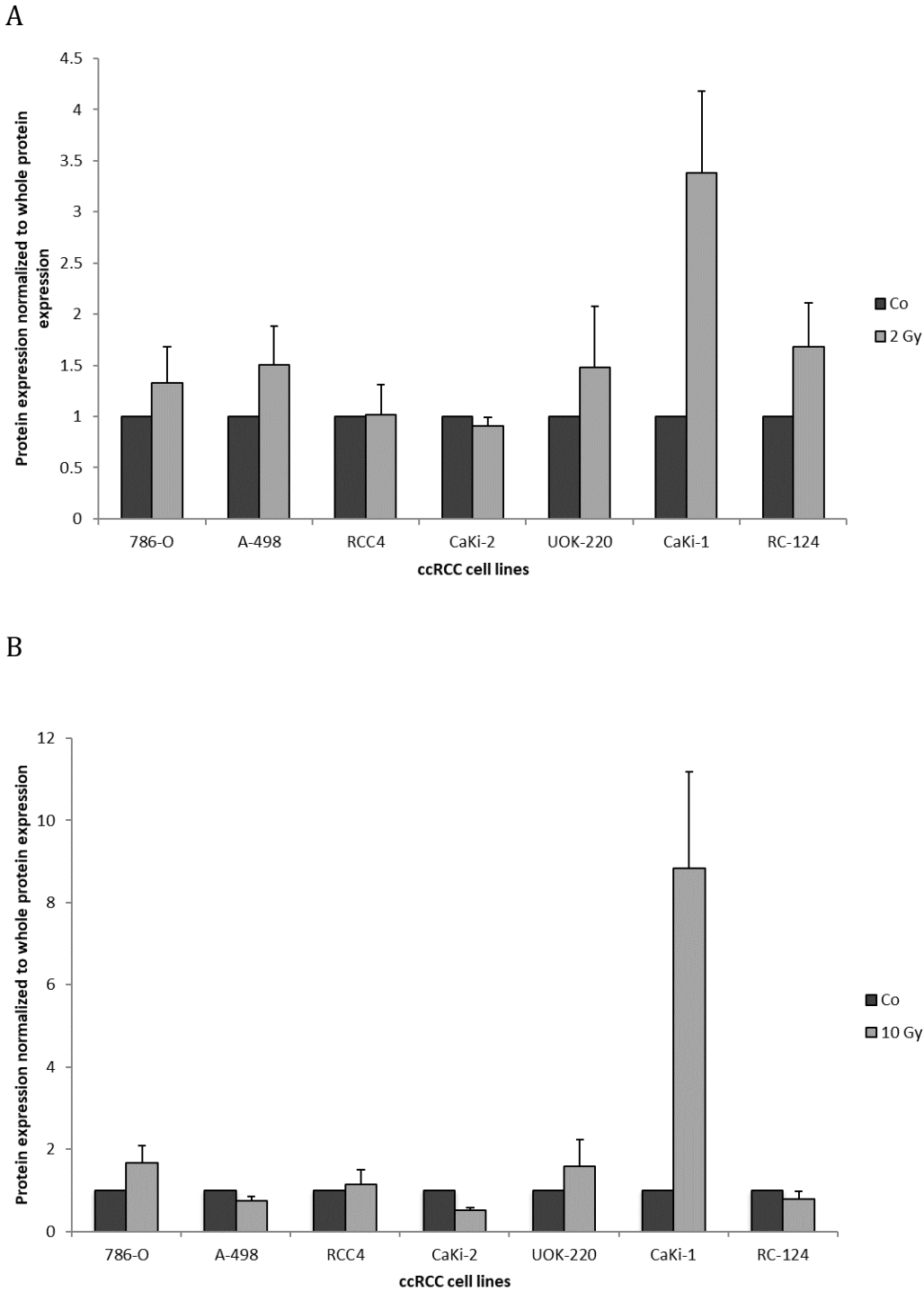


Fig. 4: Mdm2 expression in ccRCC cell lines after irradiation with (A) 2 Gy and (B) 10 Gy. Western blot was used to investigate the changes in Mdm2 expression. The data from irradiated cells is depicted in fold change relative to untreated cells. N=3. Error bars represent standard error of the mean (SEM).

3.3. Evaluating the response of the NF- κ B pathway to radiation

The response of the NF- κ B pathway to radiation was investigated. For this purpose, western blot (wet blot transfer system) and real-time polymerase chain reaction (rtPCR) were performed. Cytoplasmatic and nucleic extracts were prepared for selected cell lines in order to investigate the localization of certain NF κ B members after irradiation. The members of the NF κ B family investigated included P65, phosphorylated P65, I κ B α , phosphorylated I κ B α , IKK α / β and phosphorylated IKK α / β . Target genes investigated included the proto-oncogene c-Myc, the inflammatory cytokin IL6, and regulators of apoptosis cIAP1, cIAP2 and Bcl-xL.

Cell line HEK-293 (embryonic kidney cell line), which contains a fully functioning p53 and cell line SAOS-2, which is p53 negative, were used as a control group. Both contain a functioning VHLwt and express HIF-1 α and HIF-2 α . (47, 48)

3.3.1. I κ B α and pI κ B α

Western Blots were performed and I κ B α was analyzed after exposing all ccRCC cell lines to ionizing radiation at 2 Gy and 10 Gy. Control cell lines SAOS-2 (p53 negative) and HEK-293 (fully functioning, wild-type p53) were exposed to ionizing radiation at 10 Gy. In case of activation, a decrease in I κ B α expression would be expected.

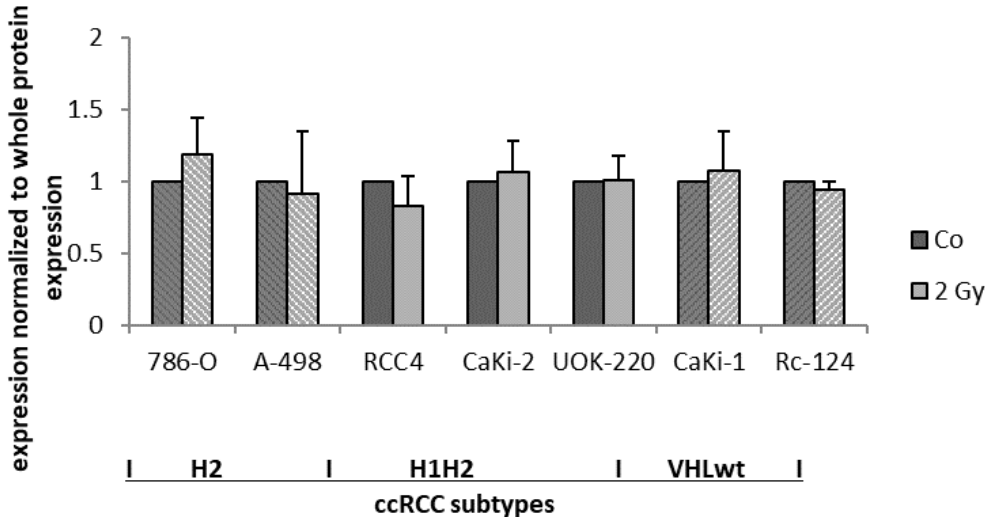
I κ B α has a mass of approximately 39 kDA. After irradiation with 2 Gy, H2 cell line 786-0 showed an increase in I κ B α , indicating that the pathway of interest had not been efficiently activated. Cell line A-498 showed a slight decrease in I κ B α . H1H2 cell lines showed minimal changes in their expression pattern, same as VHLwt cell lines: An increase could be observed in cell lines CaKi-2, UOK-220 and CaKi-1, a decrease was observed in cell lines RCC4 and Rc-124.

Irradiation of ccRCC cell lines and control cell lines SAOS-2 and HEK-293 with 10 Gy showed very much a uniform response to treatment. Cell lines of the H1H2 subtype, VHLwt cell lines and control cell lines SAOS-2 and HEK-293 all showed a decrease in I κ B α expression. A decrease in I κ B α expression was also observed in H2 cell line A-498 while an increase was only observed in H2-cell line 786-0.

The decrease of I κ B α in 8 out of 9 cell lines is a strong indicator for its degradation and thus for the efficient activation of the NF- κ B pathway after irradiation with 10 Gy.

Control cell lines HEK-293 and SAOS-2 showed a uniform response despite their difference in p53 status but showed the strongest activation process out of all our subgroups, followed by “benign” cell line Rc-124 and H1H2 cell line RCC4, while H2 cell lines showed almost no decrease in IκBα. This is depicted in fig. 5.

A



B

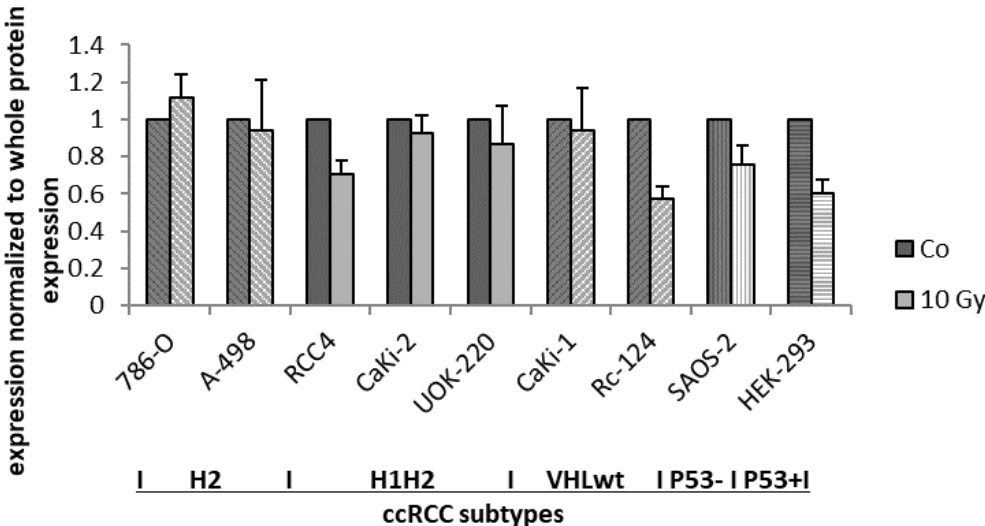


Fig. 5: IκBα expression in ccRCC cell lines, which are grouped according to their subtype (A) after irradiation with 2 Gy and (B) ccRCC cell lines, p53 negative cell line SAOS-2 and HEK-293, which contains a fully functioning p53, after irradiation with 10 Gy. Western blot was used to investigate the changes in IκBα expression. The data from irradiated cells is depicted in fold change relative to untreated cells. N=4. Error bars represent standard error of the mean (SEM).

pIκBα is the activated version of IκBα, but is quickly degraded after its phosphorylation. Due to its quick degradation after activation, our goal was to see whether it is present in

all cell lines before and after treatment. After irradiation with 2 Gy and 10 Gy, pI κ B α was detected in all ccRCC cell lines and in both control cell lines (SAOS-2 and HEK-293), as shown in fig. 6.

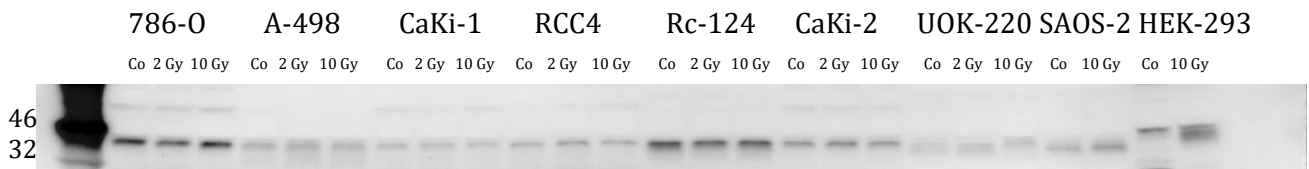


Fig. 6: Western blot showing pI κ B α expression in ccRCC cell lines 786-O, A-498, CaKi-1, RCC4, Rc-124, CaKi-2 and UOK-220, and control cell lines SAOS-2 and HEK-298 after irradiation with 2 Gy and 10 Gy.

3.3.2. IKK α / β and pIKK α / β

IKK α / β is in charge of phosphorylating I κ B α , but needs to be phosphorylated by an upstream kinase first in order to function properly. In case of an activation of the NF- κ B pathway, a decrease in the amount of IKK α / β would be expected and at the same time an increase in the amount of phosphorylated IKK α / β .

Western Blots were performed and I κ B α was analyzed after exposing all ccRCC cell lines to ionizing radiation at 2 Gy and 10 Gy. Control cell lines SAOS-2 (p53 negative) and HEK-293 (fully functioning, wild-type p53) were exposed to ionizing radiation at 10 Gy.

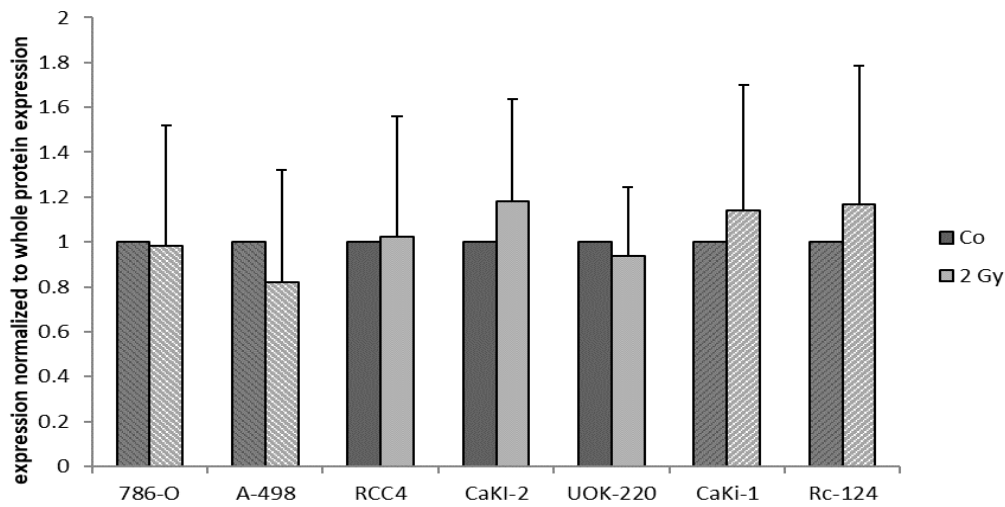
Irradiation with 2 Gy resulted in a decrease of IKK α / β in cell lines 786-O, A-498 (both subtype H2) and Rc-124 (subtype VHLwt) and in an increase of IKK α / β in cell lines RCC4, CaKi-1, UOK-220 (subtype H1H2) and CaKi-2 (subtype VHLwt).

Irradiation with 10 Gy resulted in an increase of IKK α / β in cell lines 786-O, CaKi-2, CaKi-1 and Rc-124 and in a decrease of IKK α / β in cell lines A-498, RCC4, UOK-220, SAOS-2 and HEK-293.

With the strongest decrease being seen in control cell lines SAOS-2 and HEK-293, the results of IKK α / β expression matched the results of I κ B α expression to a certain extent. H1H2 cell lines showed an increase in expression as well as H2 cell line 786-O. A-498 only showed a slight decrease within the margin of error.

Therefore, as already seen in analysis of I κ B α expression, non- ccRCC cell lines and VHL wt cell lines seem to show the strongest activation of the NF κ B pathway. The results are depicted in fig. 7.

A



B

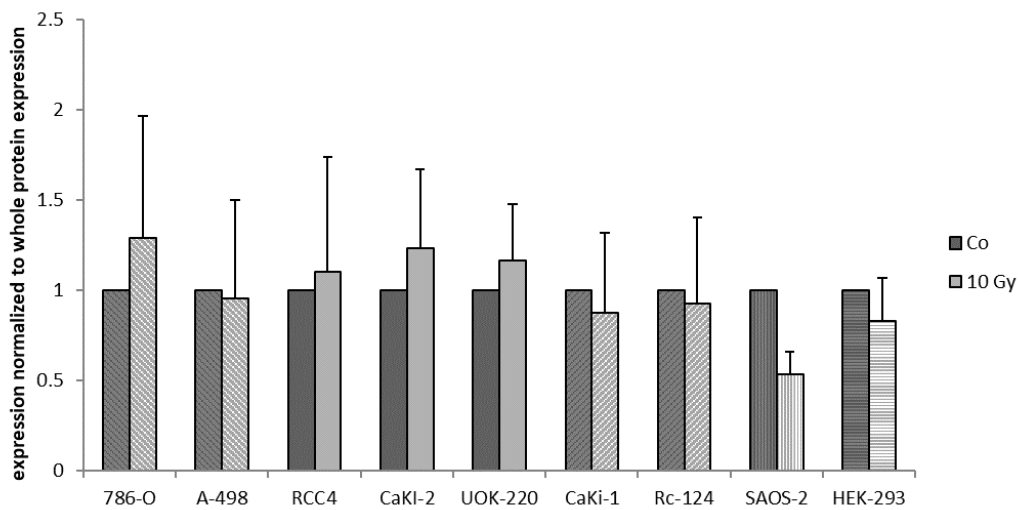


Fig. 7: IKK α/β expression in ccRCC cell lines, which are grouped according to their subtype, (A) after irradiation with 2 Gy and (B) ccRCC cell lines, p53 negative cell line SAOS-2 and HEK-293, which contains a fully functioning p53, after irradiation with 10 Gy. Western blot was used to investigate the changes in IKK α/β expression. The data from irradiated cells is depicted in fold change relative to untreated cells. N=4. Error bars represent standard error of the mean (SEM).

While the decrease is an indicator for the activation of the pathway, an increase of the phosphorylated kinase is needed simultaneously. However, phosphorylated proteins are

especially hard to detect, as they are degraded on the spot. We managed to detect pI κ B α in A-498, RCC4, Rc-124, CaKi-2 and UOK-220, as shown in fig. 8.

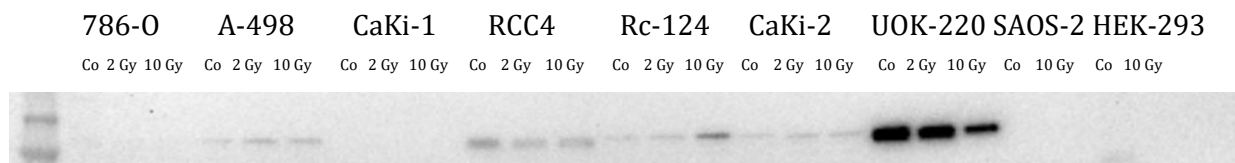


Fig. 8: Western blot showing pIKK α / expression in ccRCC cell lines 786-O, A-498, CaKi-1, RCC4, Rc-124, CaKi-2 and UOK-220, and control cell lines SAOS-2 and HEK-298 after irradiation with 2 Gy and 10 Gy.

3.3.3. P65, pP65, P105 and P50 in nucleic and cytoplasmic extracts

The mammalian NF- κ B pathway has five members, RelA (P65), RelB, c-Rel, P105/P50 (NF- κ B1) and P100/P52 (NF- κ B2). The NF- κ B proteins form homo- or heterodimers and are associated with inhibitory I κ B proteins, which prevent them from entering the nucleus. When activated, they translocate into the nucleus, where they function as transcription factors.

The experiment was conducted for selected cell lines (786-O, Rc-124, CaKi-2 and UOK-220). P65, pP65, P105 and P50 were analyzed. α -Tubulin was used as a cytoplasmic marker protein and CREB as a nucleic marker protein. Cells were irradiated with 2 Gy and 10 Gy. Afterwards, western blots were performed.

The proteins analyzed were found in the cytoplasm of all four cell lines. Only P50 was found in the nucleus. Irradiation with neither 2 Gy nor 10 Gy led to an appearance of any other protein in the nucleus. We postulated, that ccRCC cell lines might contain p50 homodimers in the nucleus, which have been known to contain antiapoptotic properties. (49) The western blots are depicted in fig. 9.

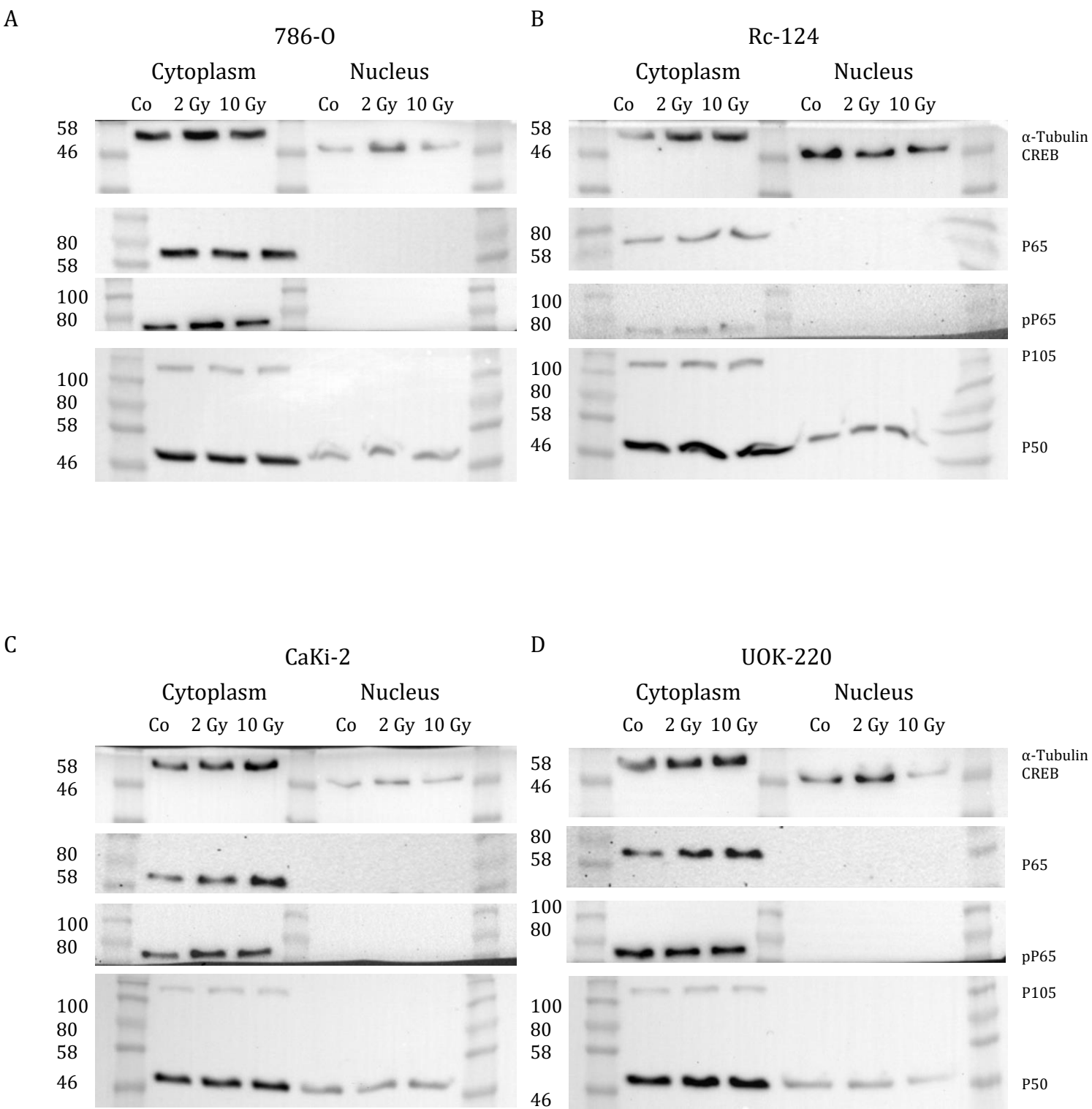


Fig. 9: Western blot demonstrating P65, pP65, P105, P50, α -Tubulin and CREB after irradiation with 2 Gy and 10 Gy in the cytosolic and nucleic fraction of ccRCC cell lines (A) 786-O (B) Rc-124 (C) CaKi-2 and (D) UOK-220: Only P50 could be detected in the nucleic fraction, P65, pP65 and P105 were only found in the cytoplasmic fraction.

3.3.4. c-Myc

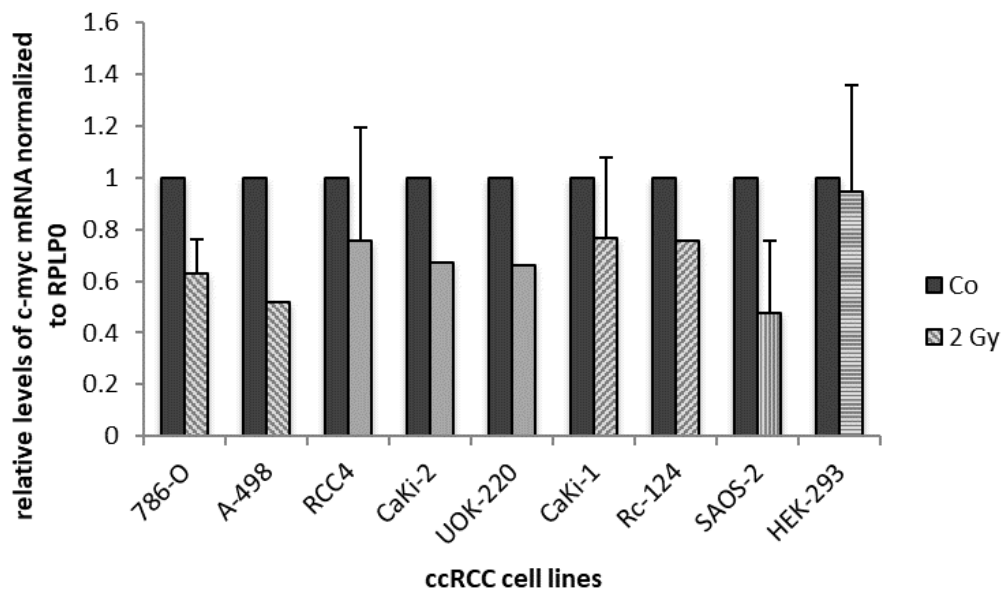
C-Myc is a gene encoding the Myc protein, which plays a crucial role in controlling cell cycle-progression and apoptosis. It does so among others by enhancing the expression of cyclins and downregulating cell cycle inhibitors such as p21 and p27. c-Myc itself is known to be inhibited by HIF-1 α and to be upregulated by HIF-2 α .

c-Myc mRNA of ccRCC cell lines 786-O, A-498, CaKi-1, RCC4, Rc-124, CaKi-2 and UOK-220 and control cell lines SAOS-2 and HEK293 was analyzed via rtPCR after irradiation with 2 Gy and 10 Gy.

Irradiation with 2 Gy resulted in a decrease of c-Myc mRNA in all cell lines, irradiation with 10 Gy resulted in a decrease of c-Myc mRNA in cell lines 786-O, A-498, CaKi-1, RCC4, Rc-124, CaKi-2 and SAOS-2 and an increase in cell lines UOK-220 and HEK-293.

The results are depicted in fig. 10.

A



B

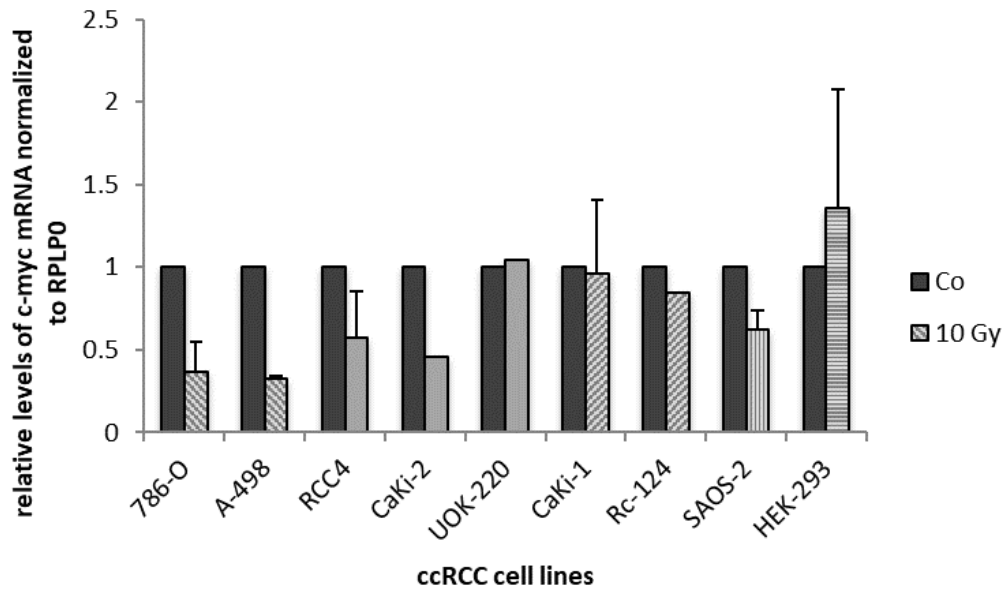


Fig. 10: c-Myc mRNA expression in ccRCC cell lines, P53 negative cell line SAOS-2 and cell line HEK-293 with fully functioning P53. Treatment was irradiation with 2 Gy (A) and 10 Gy (B). The data from irradiated cells is depicted in fold change relative to untreated cells. N=3 (786-O, SAOS-2, HEK-293), N=2 (A-498, CaKi-1, RCC4, SAOS-2), N=1 (Rc-124, CaKi-2, UOK-220). Error bars represent standard error of the mean (SEM).

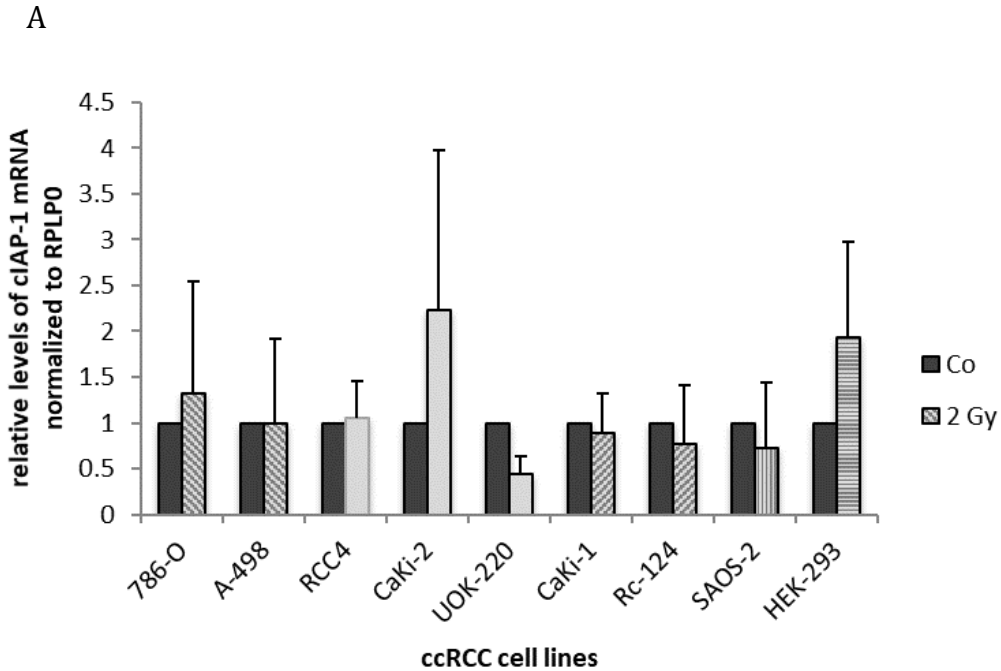
3.3.5. cIAP-1, cIAP-2, Bcl-xL

NF- κ B does not only play an important role in the cellular immune response but is also involved in the suppression of apoptosis via its target genes. These include cellular inhibitor of apoptosis-1 and 2 (cIAP-1, cIAP-2), which encode proteins of the same name, and BCL2-like 1, which encodes the anti-apoptotic Bcl-xL protein.

rtPCR of target genes cIAP-1, cIAP-2 and Bcl-xL following irradiation with 2 Gy and 10 Gy was performed in order to unravel a connection between the activation of the NF- κ B-pathway by ionizing radiation and the defective induction of apoptosis via p53 in ccRCC. Irradiation with 2 Gy led to an increase of cIAP-1 mRNA in H2 cell line 786-O, in H1H2 cell lines RCC4 and CaKi-2 and in wtP53 cell line HEK-293. Levels of mRNA didn't change in H2 cell line A-498, while a decrease was noted in both VHLwt cell lines CaKi-1 and Rc-124, in H1H2 cell line UOK-220 and in p53 negative cell line SAOS-2.

Irradiation with 10 Gy resulted in a response similar to the one described above in cell lines 786-O, RCC4, CaKi-2 and HEK-298 (increase of mRNA levels after irradiation) and

CaKi-1 (decrease of mRNA levels). Cell lines A-498 and SAOS-2 showed a (slight) decrease of mRNA levels, CaKi-1 and UOK-220 an increase of mRNA levels. The biggest increase following irradiation with 2 Gy was noticed in cell lines CaKi-2 and HEK-293 (2,3 and 2 fold). After irradiation with 10 Gy, the biggest increase was noticed in cell line CaKi-2 (3,5 fold). The results are depicted in fig. 11.



B

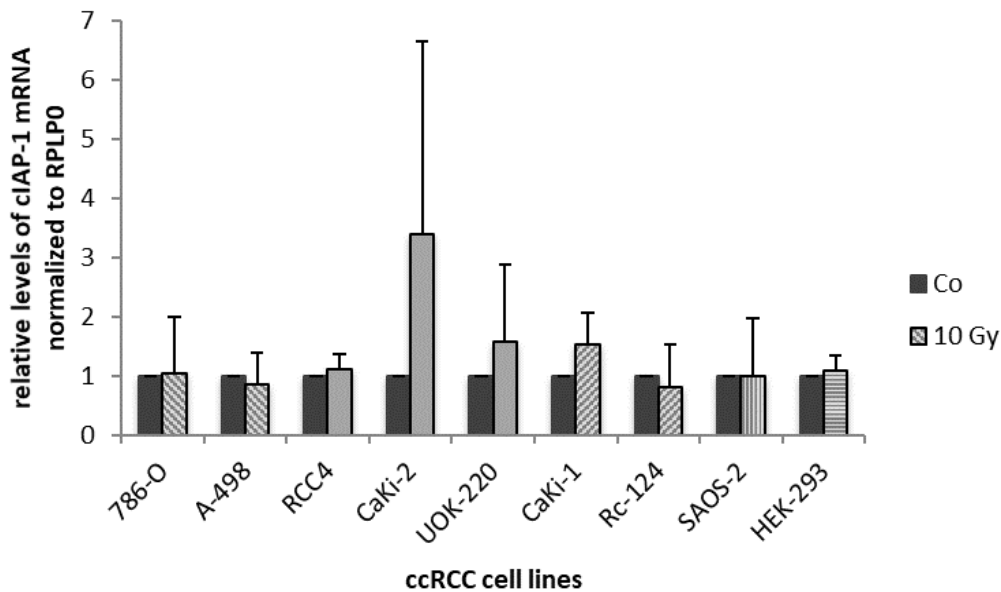


Fig. 11: cIAP-1 mRNA expression in ccRCC cell lines, P53 negative cell line SAOS-2 and cell line HEK-293 with wtP53. Treatment was irradiation with 2 Gy (A) and 10 Gy (B). The data from irradiated cells is depicted in fold change relative to untreated cells. N=3 (786-O, CaKi-1, RCC4, HEK-293), N=2 (A-498, Rc-124, CaKi-2, UOK-220, SAOS-2). Error bars represent standard error of the mean (SEM).

cIAP-2 mRNA expression was also investigated following treatment with ionizing radiation.

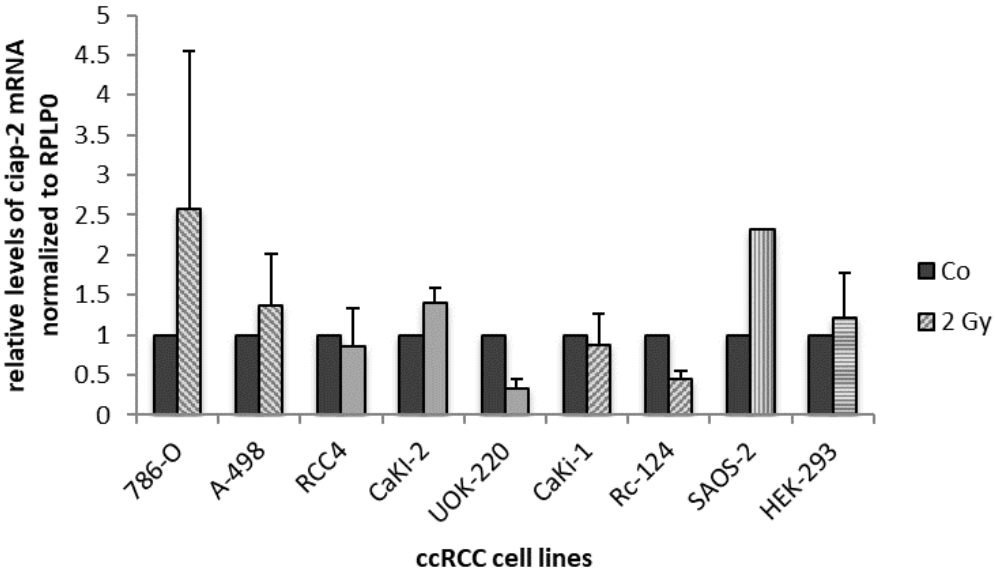
Similar results were observed with ciap-2 after irradiation with 2 Gy and 10 Gy. As with cIAP-1, an increase of mRNA was seen in cell lines 786-O, CaKi-2 and HEK-293 after irradiation with 2 Gy, in addition an increase was observed in cell lines A-498 and SAOS-2. A decrease, like with cIAP-1, was observed in cell lines CaKi-1, Rc-124 and UOK-220 and in addition in cell line RCC4. The biggest increase was observed in H2 cell line 786-O (~2,5 fold increase) and in p53- cell line SAOS-2 (~2,3 fold increase. The biggest decrease was observed in cell line Rc-124 (~0,5 fold decrease).

Following irradiation with 10 Gy, an increase was, similar to cIAP-1, noted in cell lines CaKi-1, CaKi-2, SAOS-2 and HEK-293 and in addition in cell line A-498. A decrease was observed in cell line Rc-124, and additionally in cell lines 786-O (slight decrease), RCC4, and UOK-220.

The biggest increase was noticed in both control cell lines (approximately 3 fold increase), the biggest decrease in cell lines RCC4 and Rc-124 (decreased to 1/3 and 1/5).

Overall, cIAP-2 showed a tendency of decreasing in VHLwt cell lines (two out of two cell lines after irradiation with 2 Gy, one out of two cell lines after irradiation with 10Gy). cIAP-2 increased in control cell lines after exposure to radiation, H2 cell lines showed a tendency to induce cIAP-2 mRNA expression as depicted in fig. 12.

A



B

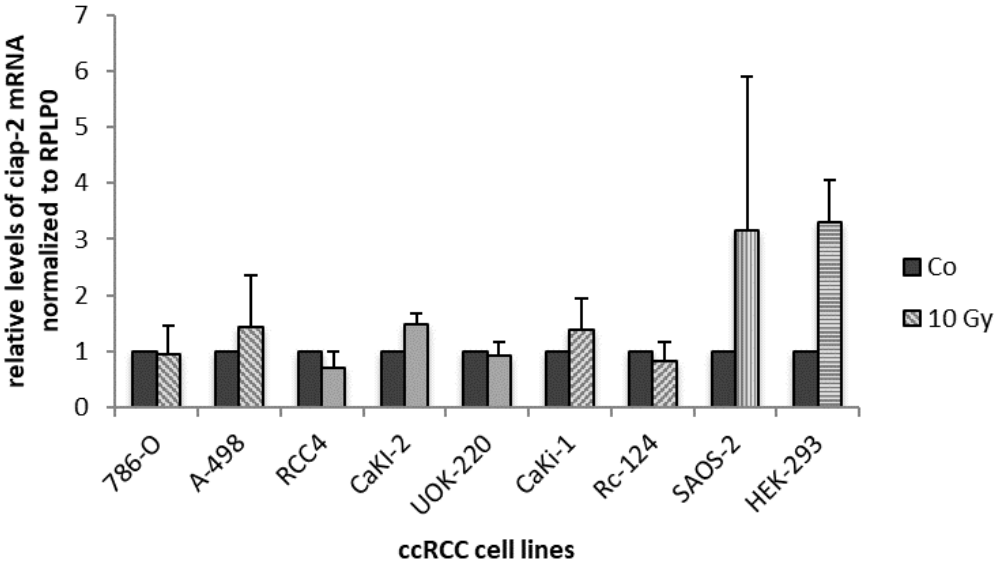


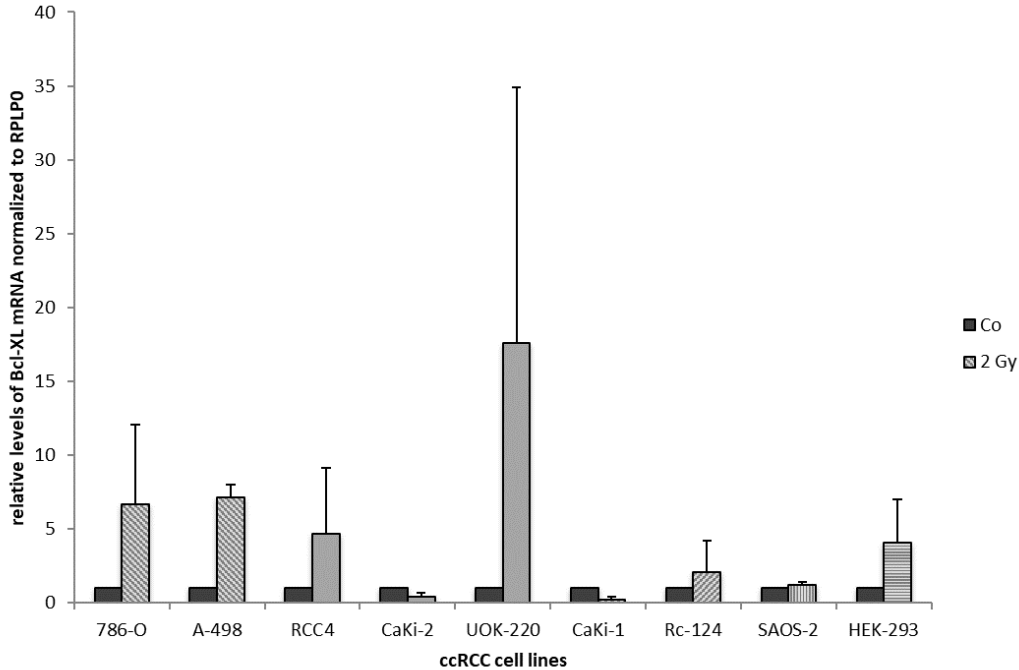
Fig. 12: cIAP-2 mRNA expression in ccRCC cell lines, P53 negative cell line SAOS-2 and cell line HEK-293 with wtP53. Treatment was irradiation with 2 Gy (A) and 10 Gy (B). The data from irradiated cells is depicted in fold change relative to untreated cells. N=3 (786-O, CaKi-1, RCC4, HEK-293), N=2 (A-498, Rc-124, CaKi-2, UOK-220, SAOS-2). Error bars represent standard error of the mean (SEM).

Bcl-xL is encoded by BCL2L1 and was the third anti-apoptotic target gene analyzed. As usual, cells were irradiated with 2 Gy and 10 Gy and RNA was extracted.

Irradiation with 2 Gy and 10 Gy led to an increase of Bcl-xL mRNA in most of the cell lines analyzed. A decrease of mRNA was only noticed in cell lines CaKi-1 and CaKi-2 after irradiation with 2 Gy and in cell lines 786-O and CaKi-1 after irradiation with 10 Gy.

The biggest increase following irradiation with 2 Gy was observed in cell lines UOK-220 (~17 fold), A-498 and A-498 (both ~7 fold). After irradiation with 10 Gy, the biggest increase was seen in cell lines UOK-220 and SOAS-2 (~60 fold and ~150 fold), as depicted in Fig. 13.

A



B

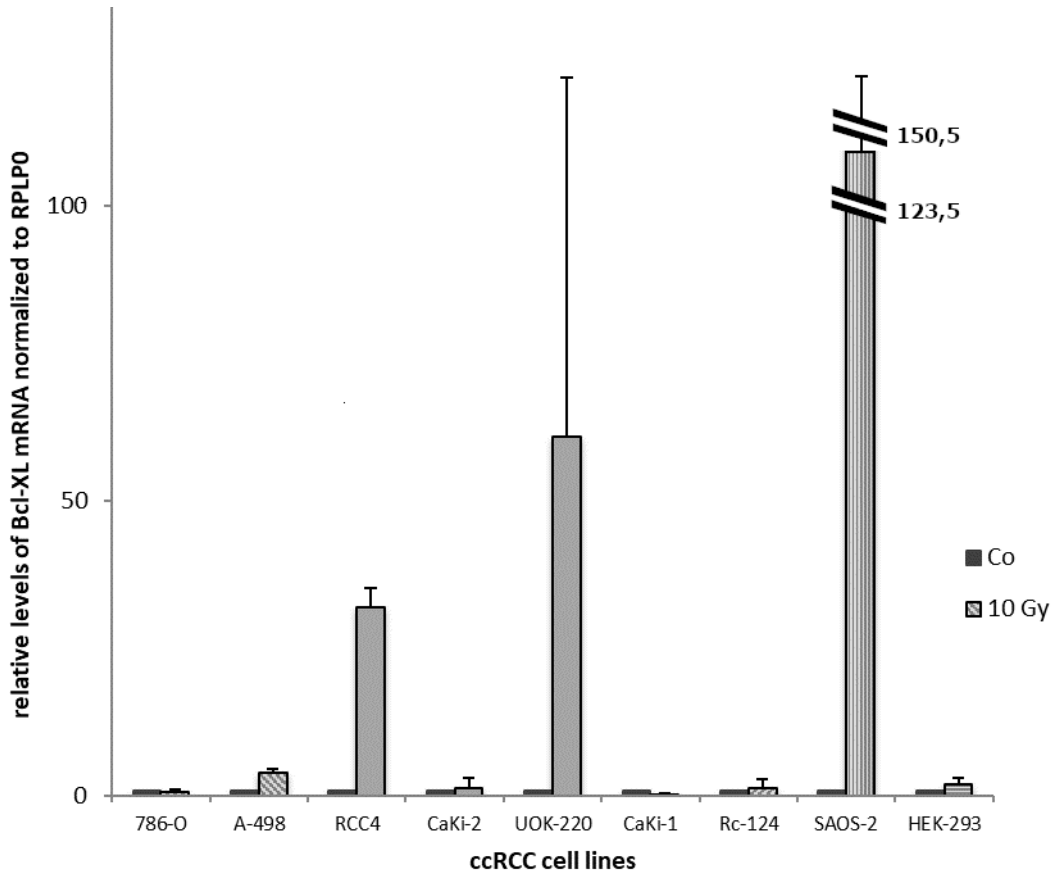


Fig. 13: Bcl-XL mRNA expression in ccRCC cell lines, P53 negative cell line SAOS-2 and cell line HEK-293 with wtP53. Treatment was irradiation with 2 Gy (A) and 10 Gy (B). The data from irradiated cells is depicted in fold change relative to untreated cells. N=3 (786-O, CaKi-1, RCC4, HEK-293), N=2 (A-498, Rc-124, CaKi-2, UOK-220, SAOS-2). Error bars represent standard error of the mean (SEM).

3.3.6. IL6

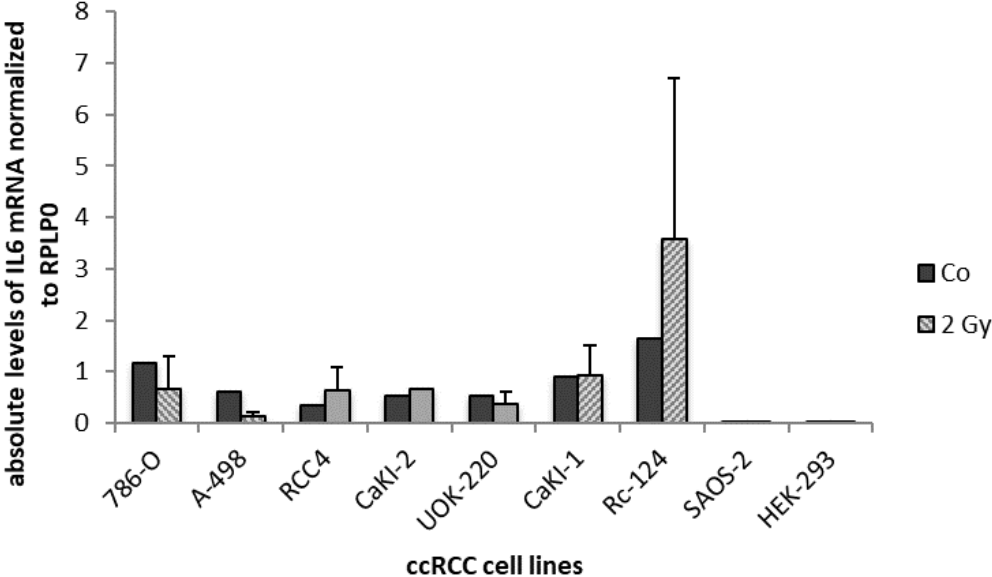
IL6 is a cytokine with both inflammatory and anti-inflammatory properties. It is encoded by the IL6-gene and activated NF- κ B proteins induce its transcription. IL6 mRNA was analyzed in order to get more information about the potential activation of the NF- κ B pathway.

Cells were irradiated and RNA was analyzed. Aside of the changes following exposure to radiation, the most astounding observation was the absolute amount of IL6 present in all cell lines: While there were decent amounts of the cytokine present in all ccRCC cell lines (e.g. 1.2 normalized fold expression in 786-O Co), it was barely measurable in the control cell lines (e. g. 0.002 normalized fold expression in HEK293 Co).

Following irradiation with 2 Gy, an increase of IL6 mRNA was noticed in H1H2 cell lines RCC4 and CaKi-2 as well as in VHLwt cell lines CaKi-1 and Rc-124. An increase following irradiation with 10 Gy was as well observed in all ccRCC cell lines except for A-498 and

Rc-124. P53 negative cell line SAOS-2 showed an increase after 2 Gy and 10 Gy, wtP53 cell line HEK-293 showed a decrease after irradiation with 2 Gy and an increase after irradiation with 10 Gy. The results are depicted in fig. 14.

A



B

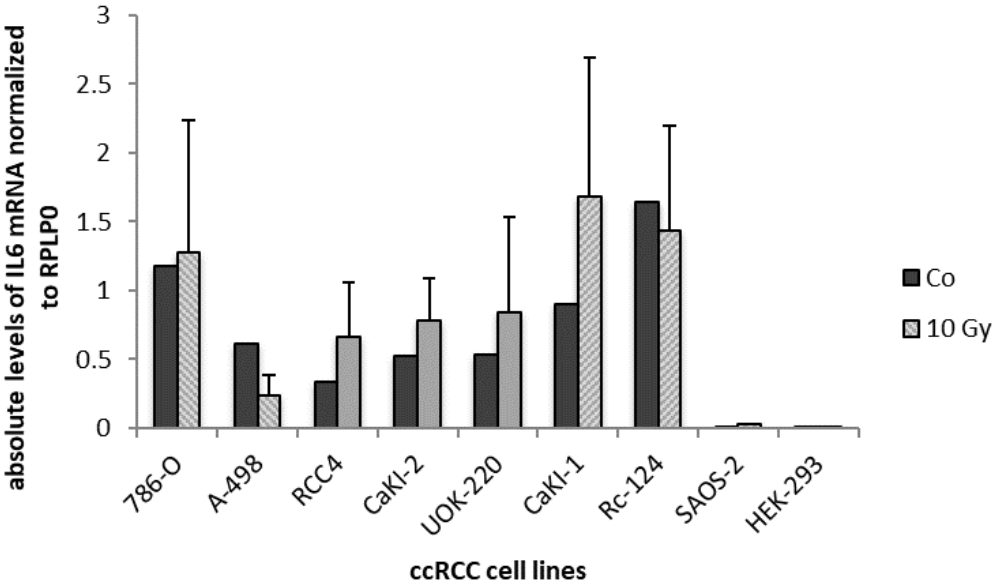


Fig. 14: IL6 mRNA expression in ccRCC cell lines, P53 negative cell line SAOS-2 and cell line HEK-293 with wtP53. Treatment was irradiation with 2 Gy (A) and 10 Gy (B). The data from irradiated cells is depicted in normalized fold expression relative to RPLP0. N=3 (786-O, CaKi-1, RCC4, HEK-293), N=2 (A-498, Rc-124, CaKi-2, UOK-220, SAOS-2). Error bars represent standard error of the mean (SEM).

4. Discussion

Personalized medicine has been a major topic for most cancer entities during the past years. However, it has become especially important for malignancies, where classic cancer therapies prove ineffective. Key element for personalized therapy is an optimal molecular characterization of the tumor. In addition, new molecular markers and a better understanding of tumorigenesis can provide insight for new therapies.

In the current study, we used RCC cell lines and one kidney cell line and were able to characterize their HIF-1 α and HIF-2 α expression pattern and therefore, we were able to assign the cell lines to one of the proposed subtypes H2, H1H2, and VHLwt.

Furthermore, we could gain insights into the behavior of the NF κ B pathway and subsequent expression of anti-apoptotic target genes among the three molecular ccRCC subtypes following irradiation. However, differences in response to irradiation in the three molecular subgroups could not be demonstrated.

4.1. Characterization of the cell lines according to their HIF-1 α and HIF-2 α expression pattern in cytoplasm and nucleus

Three cell lines (RCC4, UOK-220, CaKi-2) were assigned to subtype H1H2 and two cell lines (786-O, A-498) to subtype H2. The cell lines CaKi-1 and Rc-124 did not demonstrate either HIF subunit expression and therefore, were labeled as "VHLwt". Comparable results for several of these cell lines have been found in literature: CaKi-1 was derived from metastatic ccRCC and harbors wild-type VHL. (50) Cell line Rc-124 was derived from non-tumor kidney tissue and has not yet been characterized according to its HIF-expression pattern, but due to the tissue's origin we expect wild-type VHL, just as the findings of our experiments suggest. (51) Cell line 786-O was derived from a primary kidney tumor and harbors mutated VHL gene, while expressing solely HIF-2 α , just as cell line A-498. (18, 52) RCC4 has been described to contain mutated VHL gene while expressing both HIF-1 α and HIF-2 α . (52) Cell line UOK-220 has also been described to express both HIF-1 α and HIF-2 α while containing a mutated VHL gene. (53) There have been controversial reports about cell line CaKi-2 expressing HIF-2 α . We could detect a small staining and will thus label it as subtype H1H2, which is

supported by several experiments conducted by other work groups, but will keep in mind the possibility of it being a novel subtype “H1” (absence of HIF-2 α). (54-56)

The classification of ccRCC according to its HIF- expression pattern was initially proposed by Gordon et. al., who determined the VHL status and HIF expression in samples of ccRCCs. They found that tumors negative for HIF-1 α /-2 α had VHLwt alleles and tumors where HIF could be detected showed inactivated VHL alleles either by mutation, methylation or deletion. None of the tumors analyzed presented exclusive HIF-1 α expression and HIF- 2 α was mainly present in the nucleus. (23)

It has been proposed that HIF-2 α mainly acts as a tumor promoter while HIF-1 α has been implicated as a tumor suppressor in ccRCC. (56, 57). Consequently, Gordon et al. could demonstrate that the subtype H2 is associated with the worst prognosis.(23)

Furthermore, Kroeger et al. could confirm this finding with cytogenetic data (58) .

Therefore, the classification of the cell lines used in the current investigations according to the three molecular subtypes was an important issue that may provide new findings of these molecular ccRCC subtypes. Therapies targeting VEGF and PDGF, which are over-expressed as a result of HIF- accumulation due to loss of VHL function are an important part of today’s treatment strategy, but tumors respond very differently. Most recently, the HIF- 2 α inhibitor Belzutifan has so far been approved by the FDA for patients with von Hippel- Lindau disease. (59, 60) Furthermore, there are currently phase III clinical trials that evaluate Belzufitan in the therapy management of sporadic ccRCCs (59).

Therefore, the assignment to and consideration of the three HIF-molecular subtypes may be important for the prognostication of the prognosis of patients having ccRCC. In these current trials, ccRCC are included without consideration of the HIF-subtypes: Phase I and II trials of Belzutifan have demonstrated that not all ccRCC will respond to this substance and thus, investigations into resistance mechanisms will be required. In this regard, our classification of the cell lines used in the current study provides a basis for future in-vitro studies.

4.2. The behavior of the NF κ B- pathway following irradiation with 2 Gy and 10 Gy

4.2.1. Activation of the NF κ B pathway

The NF κ B pathway is a central regulator of immunoregulation, cell proliferation, and apoptosis. (27) Now, there are five known members of the NF κ B family: p50, p52, c-Rel,

RelA, and RelB. The heterodimer p50/p65 (Rel A) is the most common complex of NF κ B factors. It binds to DNA and regulates gene transcription in response to infection signals or genotoxic stress like UV- or gamma- irradiation. (33) Currently, there exists only preliminary knowledge about the influence of NF κ B on tumorigenesis in ccRCC, although NF κ B has been intensively studied in many other solid tumors during the past years.

Of all NF κ B family members analyzed in the current study, only P50 was found in the nucleus. P65 and P105 remained in the cytoplasm before and after irradiation. p50 is a protein that can induce context dependent anti-apoptosis, apoptosis, gene silencing, or proliferation.(49) Thus, in all cell lines the NF κ B demonstrated most likely a tendency for anti-apoptotic effects. However, according to the observed activation of the pathway this effect may be most pronounced in cell lines with VHLwt (RC-124; Caki-1). For example, the control cell lines SAOS-2 and HEK-293 showed the strongest decrease in I κ B α and IKK α / β levels following irradiation and this effect could also be observed in +VHLwt cell lines CaKi-1 and Rc-124. In contrast, H2 cell lines 786-0 and A-498 were not affected and presented virtually almost unchanged levels of I κ B α and IKK α / β . I κ B α and IKK α / β potentially decrease when the NF κ B pathway is activated.(35) This finding indicates that VHLwt cell lines (CaKi-1 and RC-124) and the control cell lines (SAOS-2 and HEK-293) most likely demonstrated the strongest NF κ B activation while H2 cell lines (786-0 and A498) were barely affected, presenting virtually unchanged levels of I κ B α and IKK α / β .

To summarize, control cell lines SAOS-2 and HEK-293 showed the strongest response to irradiation, whether it be the activation of the NF κ B pathway by demonstrating a decrease in I κ B α and IKK α / β or by presenting us with an increase of the mRNA of antiapoptotic target genes cIAP-1, cIAP-2 and Bcl- xL, which will be further examined in the following chapter.

The ccRCC cell lines didn't show a uniform response neither as a whole nor when divided into the subgroups first established in the previous chapter.

Our results of P50 being the only NF κ B member that was found in the nucleus could point towards P50 homodimers, which are known to have different characteristics than dimers that involve other NF- κ B members such as P65: Heterodimers including p50/p65, p65/p65, p65/c-rel and p50/c-rel are transcriptionally active, whereas

homodimers are most likely to repress transcription. This includes homodimers p50/p50 and p52/p52.(37)

4.2.2. Crosstalk between the NFκB pathway and p53

It has been described that there is an intensive crosstalk between the NFκB- and TP53 pathways. On the one hand, it has been demonstrated, that the NFκB pathway can activate TP53.(61) In addition it has been demonstrated, that the inhibition of this activation results in complete loss of apoptotic function of p53.(61) On the other hand, NFκB promotes transcription of anti-apoptotic genes such as Bcl-xL, c-IAP1, c-IAP2, and A1/Bfl1.(62) Moreover, it has been shown that p65 -/- mice die because of apoptotic hepatocytes.(63) Therefore, depending on the cellular situation, NFκB can either induce apoptosis or inhibit the same biological process.

For cells to transform into malignant cells, often mutations of several genes are needed. Mutation and as a result accumulation of Bcl- xL and c-Myc are often observed together.(64) C-Myc has proapoptotic as well as antiapoptotic qualities and can be seen as a link between the NFκB pathway and the p53 pathway.(65) For example it induces the protein ARF, which in return inhibits Mdm2, one of the most important negative regulators of p53. (66)

We investigated anti-apoptotic proteins that are transcriptionally activated by the NFκB pathway and are linked to anti-apoptotic effects. In addition, we looked at mRNA levels of c- Myc and investigated changes in Mdm2 protein levels following irradiation. The c- Myc levels were also of interest to us, as it has been suggested, that HIF- 1α inhibits c- Myc activity, whereas HIF- 2α might promote c- Myc activity. (23)

The antiapoptotic proteins analyzed included Bcl-xL, cIAP-1 and cIAP-2. (45, 46, 67, 68) cIAP-1 was upregulated in all H1H2 cell lines following irradiation with 10 Gy, and in RCC4 and CaCi-2 following irradiation with 2 Gy. VHLwt cell lines showed a decrease following irradiation, except for CaKi-1 after irradiation with 10 Gy, which showed an increase. Control cell lines didn't show a uniform response. cIAP-2 was upregulated in control cell lines SAOS-2 and HEK-293 following irradiation, Also H2 cell lines showed an increase following irradiation with 2 Gy but no uniform response after 10 Gy. VHLwt cell lines and H1H2 cell lines didn't show a uniform response. Bcl-xL was upregulated in control cell lines as well, but no uniform response could be detected in the other cell lines. Collectively, these results did not demonstrate a uniform trend for transcriptional

activation of anti-apoptotic proteins in ccRCC cell lines in general and the molecular subtypes VHLwt; H1H2 and H2 in particular.

C- Myc mRNA was downregulated in all cell lines following irradiation with 2 Gy and all cell lines except for UOK-220 and HEK-293 following irradiation with 10 Gy. The same reaction was observed in glioblastoma cells, which are also known to be radioresistant. (69) As the response of our control cell lines SAOS-2 and HEK-293 didn't show a significant difference however, this response does not seem to be responsible for ccRCC's resistance to radiotherapy.

Mdm2 also didn't show a uniform response following irradiation with 2 Gy and 10 Gy, especially no response that could be linked to the decline in c-Myc mRNA. Since the relationship between p53 and Mdm2 is influenced by many factors, more research is needed in this area.

4.2.3. Immunological effects of NFκB pathway

To test potential immunologically activating effects of the NFκB pathway as an explanation for potential p53 inhibition in ccRCC, real-time PCR of the NFκB target gene IL6 was conducted. IL-6 has been demonstrated to be prognostically relevant in ccRCC. (70) IL-6 is a pro-inflammatory protein. (71) In the current study, all ccRCC cell lines showed indefinitely higher absolute IL6 mRNA levels in comparison with control cell lines SAOS- 2 and HEK 293. Irradiation however didn't present us with a uniform response, especially after irradiation with only 2 Gy. Irradiation with 10 Gy showed an increase of IL6 levels in all ccRCC cell lines except for A-498 and Rc-124. Therefore, the proposed concept of biological differences in three HIF molecular subtypes could not be confirmed in this investigation.

4.2.4. Paragraph of limitations and clinical significance

Today it is clearer than ever, that even tumors of the same entity don't always share the same characteristics. Some tumors will respond to a certain therapy with complete remission, some tumors grow and spread during therapy. Some patients will experience immense, sometimes even deadly side effects. It can be challenging to predict the outcome of a therapy. We wanted to reflect this diversity with our experiments. It was the reason, why we opted to conduct our experiments with as much as nine cell lines. Not only was it our aim to establish a molecular classification of ccRCC according to its

HIF expression pattern, but we also wanted to compare cell lines within the same subtype.

While this on one hand one of the strongest assets of our research, having many cell lines to verify or dismiss results of the experiments conducted, it has also led to one of the biggest limitations our study faces.

Due to the very time-consuming process of cultivating many cell lines and preparing the various extracts for the experiments, the experiments were run only two to four times (n=2-4). The buffer for extracting nucleic and cytoplasmic extracts had to be changed and adjusted several times and the samples had to be discarded in the process, which is why the number of cell lines was downsized for this experiment.

The point of time, when the cells were harvested was determined in experiments conducted prior by Kroeger et al., however only maximum activation of p53 was considered. We cannot rule out, that NFκB activation happens after or prior to p53 activation.

Another limitation is the measurement of NFκB activity. It is common to measure the activity by analyzing the translocation of NFκB proteins into the nucleus, as presented in our experiments. However, activation can also be measured by image-based monitoring. (72) We tried this method several times, unfortunately we failed to get useful results and even with several changes to our protocol didn't manage to eliminate relevant errors. Another method for future experiments might be using a gene reporter assay. Despite these limitations, the concept of dividing clear cell Renal Cell Carcinoma according to its HIF expression pattern remains an important topic, especially in the light of the recently approved HIF-2α inhibitor Belzufen.

The significance of our finding, that only P50 seems to be present in the nucleus, remains subject to further research. Additional methods as proposed above should be used to confirm our findings. More research is needed to put this finding in context with the various functions of the NFκB pathway.

4.2.5. Summary

Clear cell renal cell carcinoma is the most frequent malignant kidney tumor in adults. It is often associated with biallelic VHL mutations. We characterized our cell lines according to their HIF expression pattern. Cell lines RCC4, UOK-220 and CaKi-2 were assigned to subtype H1H2, cell lines 786-O and A-498 were assigned to subtype H2 and cell lines CaKi-1 and Rc-124 were assigned to subtype VHLwt.

Previous work of our group had shown, that p53 can be activated in ccRCC following irradiation but is not able to induce apoptosis. An important link to p53 activity with strong antiapoptotic qualities is the NF κ B pathway, which can be activated e. g. by irradiation.

We irradiated the three subtypes previously established as well as two control cell lines, SAOS-2 (p53 negative cell line) and HEK 293 (contains functioning p53) with 2 Gy and 10 Gy and analyzed several proteins of the pathway by using western blots. Several target genes with antiapoptotic qualities were analyzed by using rt-PCR.

We found, that out of the cell lines analyzed, both control cell lines (SAOS-2, HEK 293) showed the strongest response (activation of the NF κ B pathway) following irradiation. Among the three ccRCC subtypes the VHLwt cell lines showed the strongest response. H2 cell lines showed almost no response at all.

A connection between the missing ability of p53 to induce apoptosis and an induction of transcription factors by the NF κ B pathway could not be determined. We also could not determine biological differences between the subtypes.

We analyzed, whether any NF κ B proteins were present in the nucleus following irradiation and found, that only p50 homodimers were present in the nucleus. This might point towards p50 homodimers, which have been described to have different characteristics than heterodimers. More research is needed to analyze this important finding.

5. Bibliography

1. Registries ENoC. Kidney cancer (KC) factsheet. ENCR Factsheets. 2017.
2. Gesellschaft RK-IHud, (Hrsg) deKiDeV. Niere. Krebs in Deutschland für 2013/2014
2017:100-3.
3. Lee CT, Katz J, Fearn PA, Russo P. Mode of presentation of renal cell carcinoma provides prognostic information. *Urologic oncology*. 2002;7(4):135-40.
4. Petejova N, Martinek A. Renal cell carcinoma: Review of etiology, pathophysiology and risk factors. *Biomedical papers of the Medical Faculty of the University Palacky, Olomouc, Czechoslovakia*. 2016;160(2):183-94.
5. Jonasch E, Gao J, Rathmell WK. Renal cell carcinoma. *BMJ (Clinical research ed)*. 2014;349:g4797.
6. Motzer RJ, Mazumdar M, Bacik J, Berg W, Amsterdam A, Ferrara J. Survival and prognostic stratification of 670 patients with advanced renal cell carcinoma. *Journal of clinical oncology : official journal of the American Society of Clinical Oncology*. 1999;17(8):2530-40.
7. Motzer RJ, Bacik J, Murphy BA, Russo P, Mazumdar M. Interferon-alfa as a comparative treatment for clinical trials of new therapies against advanced renal cell carcinoma. *Journal of clinical oncology : official journal of the American Society of Clinical Oncology*. 2002;20(1):289-96.
8. Motzer RJ, Russo P, Nanus DM, Berg WJ. Renal cell carcinoma. *Current problems in cancer*. 1997;21(4):185-232.
9. (DGU) DGfUeV. Kurzversion S3-Leitlinie Nierenzellkarzinom. Leitlinienprogramm Onkologie. 2017.
10. Amato RJ. Chemotherapy for renal cell carcinoma. *Seminars in oncology*. 2000;27(2):177-86.
11. Tunio MA, Hashmi A, Rafi M. Need for a new trial to evaluate postoperative radiotherapy in renal cell carcinoma: a meta-analysis of randomized controlled trials. *Annals of oncology : official journal of the European Society for Medical Oncology*. 2010;21(9):1839-45.
12. Bedke J, Gauler T, Grunwald V, Hegele A, Herrmann E, Hinz S, et al. Systemic therapy in metastatic renal cell carcinoma. *World journal of urology*. 2017;35(2):179-88.
13. Patel PH, Chadalavada RS, Chaganti RS, Motzer RJ. Targeting von Hippel-Lindau pathway in renal cell carcinoma. *Clinical cancer research : an official journal of the American Association for Cancer Research*. 2006;12(24):7215-20.
14. Motzer RJ, Hutson TE, Tomczak P, Michaelson MD, Bukowski RM, Oudard S, et al. Overall survival and updated results for sunitinib compared with interferon alfa in patients with metastatic renal cell carcinoma. *Journal of clinical oncology : official journal of the American Society of Clinical Oncology*. 2009;27(22):3584-90.
15. Rini BI, McDermott DF, Hammers H, Bro W, Bukowski RM, Faba B, et al. Society for Immunotherapy of Cancer consensus statement on immunotherapy for the treatment of renal cell carcinoma. *Journal for immunotherapy of cancer*. 2016;4:81.
16. Atkins MB, Tannir NM. Current and emerging therapies for first-line treatment of metastatic clear cell renal cell carcinoma. *Cancer treatment reviews*. 2018;70:127-37.
17. Maher ER, Kaelin WG, Jr. von Hippel-Lindau disease. *Medicine*. 1997;76(6):381-91.

18. Maxwell PH, Wiesener MS, Chang GW, Clifford SC, Vaux EC, Cockman ME, et al. The tumour suppressor protein VHL targets hypoxia-inducible factors for oxygen-dependent proteolysis. *Nature*. 1999;399(6733):271-5.
19. Nickerson ML, Jaeger E, Shi Y, Durocher JA, Mahurkar S, Zaridze D, et al. Improved identification of von Hippel-Lindau gene alterations in clear cell renal tumors. *Clinical cancer research : an official journal of the American Association for Cancer Research*. 2008;14(15):4726-34.
20. Comprehensive molecular characterization of clear cell renal cell carcinoma. *Nature*. 2013;499(7456):43-9.
21. Li L, Kaelin WG, Jr. New insights into the biology of renal cell carcinoma. *Hematology/oncology clinics of North America*. 2011;25(4):667-86.
22. Gordan JD, Thompson CB, Simon MC. HIF and c-Myc: sibling rivals for control of cancer cell metabolism and proliferation. *Cancer cell*. 2007;12(2):108-13.
23. Gordan JD, Lal P, Dondeti VR, Letrero R, Parekh KN, Oquendo CE, et al. HIF-alpha effects on c-Myc distinguish two subtypes of sporadic VHL-deficient clear cell renal carcinoma. *Cancer cell*. 2008;14(6):435-46.
24. Vogelstein B, Lane D, Levine AJ. Surfing the p53 network. *Nature*. 2000;408(6810):307-10.
25. Alarcon-Vargas D, Ronai Z. p53-Mdm2--the affair that never ends. *Carcinogenesis*. 2002;23(4):541-7.
26. Wu X, Bayle JH, Olson D, Levine AJ. The p53-mdm-2 autoregulatory feedback loop. *Genes & development*. 1993;7(7a):1126-32.
27. Puszynski K, Bertolusso R, Lipniacki T. Crosstalk between p53 and nuclear factor- κ B systems: pro- and anti-apoptotic functions of NF- κ B. *IET systems biology*. 2009;3(5):356-67.
28. Kandoth C, McLellan MD, Vandin F, Ye K, Niu B, Lu C, et al. Mutational landscape and significance across 12 major cancer types. *Nature*. 2013;502(7471):333-9.
29. Sejima T, Miyagawa I. Expression of bcl-2, p53 oncoprotein, and proliferating cell nuclear antigen in renal cell carcinoma. *European urology*. 1999;35(3):242-8.
30. Gurova KV, Hill JE, Razorenova OV, Chumakov PM, Gudkov AV. p53 pathway in renal cell carcinoma is repressed by a dominant mechanism. *Cancer research*. 2004;64(6):1951-8.
31. Noon AP, Vlatkovic N, Polanski R, Maguire M, Shawki H, Parsons K, et al. p53 and MDM2 in renal cell carcinoma: biomarkers for disease progression and future therapeutic targets? *Cancer*. 2010;116(4):780-90.
32. Baldwin AS, Jr. The NF-kappa B and I kappa B proteins: new discoveries and insights. *Annual review of immunology*. 1996;14:649-83.
33. Baeuerle PA, Henkel T. Function and activation of NF-kappa B in the immune system. *Annual review of immunology*. 1994;12:141-79.
34. Libermann TA, Baltimore D. Activation of interleukin-6 gene expression through the NF-kappa B transcription factor. *Molecular and cellular biology*. 1990;10(5):2327-34.
35. Oeckinghaus A, Ghosh S. The NF-kappaB family of transcription factors and its regulation. *Cold Spring Harbor perspectives in biology*. 2009;1(4):a000034.
36. Alfred J. Robinson EJM. Transcriptional and epigenetic mechanisms of addiction. *Nature Reviews Neuroscience*. 2011;12(11):623-37.
37. Ghosh S, May MJ, Kopp EB. NF-kappa B and Rel proteins: evolutionarily conserved mediators of immune responses. *Annual review of immunology*. 1998;16:225-60.

38. Hayden MS, Ghosh S. Signaling to NF-kappaB. *Genes & development*. 2004;18(18):2195-224.
39. Neumann M, Grieshammer T, Chuvpilo S, Kneitz B, Lohoff M, Schimpl A, et al. RelA/p65 is a molecular target for the immunosuppressive action of protein kinase A. *The EMBO journal*. 1995;14(9):1991-2004.
40. Naumann M, Scheidereit C. Activation of NF-kappa B in vivo is regulated by multiple phosphorylations. *The EMBO journal*. 1994;13(19):4597-607.
41. Wu H, Lozano G. NF-kappa B activation of p53. A potential mechanism for suppressing cell growth in response to stress. *The Journal of biological chemistry*. 1994;269(31):20067-74.
42. Bohuslav J, Chen LF, Kwon H, Mu Y, Greene WC. p53 induces NF-kappaB activation by an IkappaB kinase-independent mechanism involving phosphorylation of p65 by ribosomal S6 kinase 1. *The Journal of biological chemistry*. 2004;279(25):26115-25.
43. Gurova KV, Hill JE, Guo C, Prokvolit A, Burdelya LG, Samoylova E, et al. Small molecules that reactivate p53 in renal cell carcinoma reveal a NF-kappaB-dependent mechanism of p53 suppression in tumors. *Proceedings of the National Academy of Sciences of the United States of America*. 2005;102(48):17448-53.
44. Stehlik C, de Martin R, Kumabashiri I, Schmid JA, Binder BR, Lipp J. Nuclear factor (NF)-kappaB-regulated X-chromosome-linked iap gene expression protects endothelial cells from tumor necrosis factor alpha-induced apoptosis. *The Journal of experimental medicine*. 1998;188(1):211-6.
45. Stehlik C, de Martin R, Binder BR, Lipp J. Cytokine induced expression of porcine inhibitor of apoptosis protein (iap) family member is regulated by NF-kappa B. *Biochemical and biophysical research communications*. 1998;243(3):827-32.
46. Chen C, Edelstein LC, Gelinis C. The Rel/NF-kappaB family directly activates expression of the apoptosis inhibitor Bcl-x(L). *Molecular and cellular biology*. 2000;20(8):2687-95.
47. Abd-Aziz N, Stanbridge EJ, Shafee N. Bortezomib attenuates HIF-1- but not HIF-2-mediated transcriptional activation. *Oncology letters*. 2015;10(4):2192-6.
48. Hu CJ, Wang LY, Chodosh LA, Keith B, Simon MC. Differential roles of hypoxia-inducible factor 1alpha (HIF-1alpha) and HIF-2alpha in hypoxic gene regulation. *Molecular and cellular biology*. 2003;23(24):9361-74.
49. Yu Y, Wan Y, Huang C. The biological functions of NF-kappaB1 (p50) and its potential as an anti-cancer target. *Current cancer drug targets*. 2009;9(4):566-71.
50. Trotta AM, Santagata S, Zanotta S, D'Alterio C, Napolitano M, Rea G, et al. Mutated Von Hippel-Lindau-renal cell carcinoma (RCC) promotes patients specific natural killer (NK) cytotoxicity. *Journal of experimental & clinical cancer research : CR*. 2018;37(1):297.
51. GmbH CCLS. Origin and General Characteristics, Designation: RC-124.
52. Raval RR, Lau KW, Tran MG, Sowter HM, Mandriota SJ, Li JL, et al. Contrasting properties of hypoxia-inducible factor 1 (HIF-1) and HIF-2 in von Hippel-Lindau-associated renal cell carcinoma. *Molecular and cellular biology*. 2005;25(13):5675-86.
53. Sourbier C, Srivastava G, Ghosh MC, Ghosh S, Yang Y, Gupta G, et al. Targeting HIF2 α translation with Tempol in VHL-deficient clear cell renal cell carcinoma. *Oncotarget*. 2012;3(11):1472-82.
54. Wohlrab C, Kuiper C, Vissers MC, Phillips E, Robinson BA, Dachs GU. Ascorbate modulates the hypoxic pathway by increasing intracellular activity of the HIF hydroxylases in renal cell carcinoma cells. *Hypoxia (Auckland, NZ)*. 2019;7:17-31.

55. Brodaczewska KK, Szczylik C, Fiedorowicz M, Porta C, Czarnecka AM. Choosing the right cell line for renal cell cancer research. *Molecular cancer*. 2016;15(1):83.
56. Shen C, Beroukhi R, Schumacher SE, Zhou J, Chang M, Signoretti S, et al. Genetic and functional studies implicate HIF1 α as a 14q kidney cancer suppressor gene. *Cancer discovery*. 2011;1(3):222-35.
57. Czyzyk-Krzeska MF, Landero Figueroa JA, Gulati S, Cunningham JT, Meller J, Shamsae IB, et al. Molecular and Metabolic Subtypes in Sporadic and Inherited Clear Cell Renal Cell Carcinoma. *Genes*. 2021;12(3).
58. Kroeger N, Klatter T, Chamie K, Rao PN, Birkhäuser FD, Sonn GA, et al. Deletions of chromosomes 3p and 14q molecularly subclassify clear cell renal cell carcinoma. *Cancer*. 2013;119(8):1547-54.
59. Choueiri TK, Kaelin WG, Jr. Targeting the HIF2-VEGF axis in renal cell carcinoma. *Nature medicine*. 2020;26(10):1519-30.
60. Jonasch E, Donskov F, Iliopoulos O, Rathmell WK, Narayan VK, Maughan BL, et al. Belzutifan for Renal Cell Carcinoma in von Hippel-Lindau Disease. *The New England journal of medicine*. 2021;385(22):2036-46.
61. Ryan KM, Ernst MK, Rice NR, Vousden KH. Role of NF-kappaB in p53-mediated programmed cell death. *Nature*. 2000;404(6780):892-7.
62. Barkett M, Gilmore TD. Control of apoptosis by Rel/NF-kappaB transcription factors. *Oncogene*. 1999;18(49):6910-24.
63. Beg AA, Sha WC, Bronson RT, Ghosh S, Baltimore D. Embryonic lethality and liver degeneration in mice lacking the RelA component of NF-kappa B. *Nature*. 1995;376(6536):167-70.
64. Vaux DL, Cory S, Adams JM. Bcl-2 gene promotes haemopoietic cell survival and cooperates with c-myc to immortalize pre-B cells. *Nature*. 1988;335(6189):440-2.
65. Fairlie WD, Lee EF. Co-Operativity between MYC and BCL-2 Pro-Survival Proteins in Cancer. *International journal of molecular sciences*. 2021;22(6).
66. Feng YC, Liu XY, Teng L, Ji Q, Wu Y, Li JM, et al. c-Myc inactivation of p53 through the pan-cancer lncRNA MILIP drives cancer pathogenesis. *Nature communications*. 2020;11(1):4980.
67. Salvesen GS, Duckett CS. IAP proteins: blocking the road to death's door. *Nature reviews Molecular cell biology*. 2002;3(6):401-10.
68. Chu ZL, McKinsey TA, Liu L, Gentry JJ, Malim MH, Ballard DW. Suppression of tumor necrosis factor-induced cell death by inhibitor of apoptosis c-IAP2 is under NF-kappaB control. *Proceedings of the National Academy of Sciences of the United States of America*. 1997;94(19):10057-62.
69. Rodrigues PMG, de Souza RS, Borges HL, Martins RAP. Regulation of c-Myc and NBS1 by ionizing radiation in glioblastoma cells. *Oncology Signaling*. 2018;1(1):1-5.
70. Fu Q, Chang Y, An H, Fu H, Zhu Y, Xu L, et al. Prognostic value of interleukin-6 and interleukin-6 receptor in organ-confined clear-cell renal cell carcinoma: a 5-year conditional cancer-specific survival analysis. *British journal of cancer*. 2015;113(11):1581-9.
71. Jones SA. Directing transition from innate to acquired immunity: defining a role for IL-6. *Journal of immunology (Baltimore, Md : 1950)*. 2005;175(6):3463-8.
72. Ernst O, Vayttaden SJ, Fraser IDC. Measurement of NF- κ B Activation in TLR-Activated Macrophages. *Methods in molecular biology (Clifton, NJ)*. 2018;1714:67-78.

Eidesstattliche Erklärung

Hiermit erkläre ich, dass ich die vorliegende Dissertation selbständig verfasst und keine anderen als die angegebenen Hilfsmittel benutzt habe.

Die Dissertation ist bisher keiner anderen Fakultät, keiner anderen wissenschaftlichen Einrichtung vorgelegt worden.

Ich erkläre, dass ich bisher kein Promotionsverfahren erfolglos beendet habe und dass eine Aberkennung eines bereits erworbenen Doktorgrades nicht vorliegt.

Datum

Unterschrift

Declaration of Originality

I confirm that the submitted thesis is original work and was written by me without further assistance. Appropriate credit has been given where reference has been made to the work of others. The thesis was not examined before, nor has it been published. The submitted electronic version of the thesis matches the printed version.

Date

Signature